Available online at www.sciencedirect.com

SCIENCE DIRECT®

Biochimica et Biophysica Acta 1666 (2004) 205–226

BIOCHIMICA ET BIOPHYSICA ACTA
BBA

http://www.elsevier.com/locate/bba

Review

Lipids do influence protein function—the hydrophobic matching hypothesis revisited

Morten Ø. Jensen, Ole G. Mouritsen*

MEMPHYS-Center for Biomembrane Physics, University of Southern Denmark, Campusvej 55, DK-5230 Odense M, Denmark

Received 1 April 2004; received in revised form 28 May 2004; accepted 24 June 2004
Available online 23 July 2004

Abstract

A topical review of the current state of lipid–protein interactions is given with focus on the physical interactions between lipids and integral proteins in lipid-bilayer membranes. The concepts of hydrophobic matching and curvature stress are revisited in light of recent data obtained from experimental and theoretical studies which demonstrate that not only do integral proteins perturb the lipids, but the physical state of the lipids does also actively influence protein function. The case of the trans-membrane water-channel protein aquaporin GlpF from *E. coli* imbedded in lipid-bilayer membranes is discussed in some detail. Numerical data obtained from Molecular Dynamics simulations show on the one side that the lipid bilayer adapts to the channel by a hydrophobic matching condition which reflects the propensity of the lipid molecules for forming curved structures. On the other side, it is demonstrated that the transport function of the channel is modulated by the matching condition and/or the curvature stress in a lipid-specific manner.

Keywords: Lipid bilayer; Integral membrane protein; Hydrophobic thickness; Lipid domain; Membrane raft; Hydrophobic matching; Structure–function relationship; Trans-membrane peptide; Gramicidin A; Curvature stress; Protein folding; Protein insertion; Theory of lipid–protein interactions; Water channel protein; Molecular Dynamics; Lipid order parameter; Chain tilt; Water transport

Contents

Abbreviations: DAPC, di-arachioyl phosphatidylcholine; DLPC, di-laureoyl phosphatidylcholine; DMPC, di-myristoyl phosphatidylcholine; DOPC, di-oleoyl phosphatidylcholine; DPPC, di-palmitoyl phosphatidylcholine; DPPE, di-palmitoyl phosphatidylcholine; DSPC, di-stearoyl phosphatidylcholine; PC, phosphatidylcholine; PE, phosphatidylethanolamine; POPE, 16:0/18:1c9-palmitoyloleyl phosphatidylethanolamine; POPC, 16:0/18:1c9-palmitoyloleyl phosphatidylcholine; SM, sphingomyelin

* Corresponding author. Tel.: +45 65 653 528; fax: +45 66 158 760.
E-mail address: ogm@memphys.sdu.dk (O.G. Mouritsen).

0005-2736/$ - see front matter © 2004 Elsevier B.V. All rights reserved.
doi:10.1016/j.bbamem.2004.06.009

1. Introduction

One would have expected that the study of lipid–protein interactions in membranes had come a long way since Erich Sackmann[1] two decades ago in 1984 [1] suggested that the function of integral membrane proteins may be triggered by the lipid-bilayer properties as illustrated by the picture in Fig. 1. Already this picture anticipated the possibility that the local lipid environment around a membrane protein may have quite different properties from those that characterize the average, global state of the membrane, e.g., in terms of varying molecular composition, curvature, or hydrophobic thickness. In 1984, the field of lipid–protein interactions still enjoyed a strong activity. Singer and Nicolson [2] had in 1972 placed mobile trans-membrane proteins in the fluid-mosaic model of the membrane and Israelachvili [3] had in his refinements of the fluid-mosaic model from 1977 anticipated that lipids and proteins interact via the structural and morphological properties of the lipid bilayer. However, after years of heated activity in the field during the seventies and early eighties, to a large extent fuelled by the somewhat futile discussion among spectroscopists about the possibly existence of a lipid annulus, the field of lipid–protein interactions was abandoned by many scientists and left as an esoteric discipline for a small group of dedicated, non-mainstream scientists. Several events in recent years have, however, changed the status of the field considerably. The field is becoming fashionable again.

After the big quest for the Holy Grail of the genome, it has become painstakingly clear to many researchers that the genome is not the whole answer. A conventional molecular biology approach to the most difficult problems in membrane and cell biology has to be supplemented by biophysical techniques that can uncover those macromolecular organization principles which can nowhere be read off from the genome. The genome is only the beginning of the story. The question still remains as to how cellular and subcellular structures of enormous complexity are formed out of their molecular building blocks, and how living systems are organized, regulated, and ultimately function. The old problem of bridging the gap between the genotype and phenotype remains: complete knowledge of a genome does not permit predictions about the supramolecular organization and functioning of a complex biological system. Solving this problem is far more difficult than determining the genome of a species. For this purpose, principles from fundamental physics are called for.

These general considerations apply particularly to the field of lipid–protein interactions. How do proteins influence lipids, and how do the lipids influence the proteins? The answer to these questions is not chemistry. It rather presupposes that the system of lipids and proteins are considered as a complex macromolecular aggregate, and the clarity of the answer will ultimately rely on our understanding of the physical interactions of the combined system. Hence, after decades of focus on genes and proteins, lipids are back on the scene [96]. This is perhaps most clearly expressed in the title of a recent paper by Hilgemann in Annual Reviews of Physiology entitled ‘Getting Ready for the Decade of the Lipids’ [4].

A number of circumstances forecast new developments and possible breakthroughs in the field of lipid–protein interactions: (1) First, a major result of the genome projects has been the finding that more than 30% of the genome codes for trans-membrane proteins, thereby shifting the attention towards this class of proteins. (2) Second, the advent of new and more powerful experimental and theoretical approaches, in particular, geared towards investigations on the nanometer and submicron scales, including atomic force microscopy [5,6] fluorescence microscopy [7,8], and single-molecule experiments [9,10], has shed new light on the details of lipid–protein interactions. (3) Third, molecular biology techniques can now routinely be used to express many membrane proteins and produce them in sufficiently large amounts to permit quantitative physical studies. (4) Finally, the latest hype in membrane biology

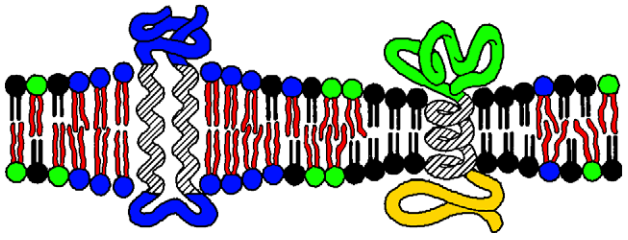

Fig. 1. Schematic illustration of triggering the function of an integral membrane protein by changing the hydrophobic mismatch. Adapted from Ref. [1].

[1] The present paper is dedicated to Erich Sackmann on the occasion of his retirement and in recognition of his seminal contributions to membrane science in general and to the field of lipid–protein interactions in particular.

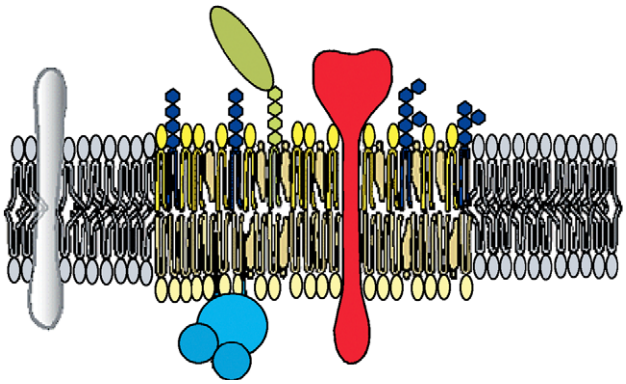

Fig. 2. Schematic illustration of a membrane raft, consisting of a lipid patch enriched in sphingolipids, glycolipids, and cholesterol to which certain proteins are attached. Adapted from www.glycoforum.gr.jp/science/word/glycolipid/GLD01E.html.

focussing on membrane structure and function in terms of so-called 'rafts' [11,12] has renewed the interest in coming to grips with one of the most difficult problems in membrane biology concerning the lateral molecular organization in the plane of the membrane and the importance of this organization for e.g., signaling, growth, and ligand–receptor interactions. It is interesting to compare Sackmann's visionary schematic cartoon from 1984 shown in Fig. 1 with a canonical picture of a so-called membrane 'raft' from 2004 as shown in Fig. 2. The similarity is striking and thought-provoking. It may either suggest that the reinvention time in membrane biology is about two decades or that Sackmann was particularly visionary.

2. Small-scale lipid membrane structure—a key to lipid–protein interactions

A detailed understanding and a quantitative characterization of the interaction between lipids and proteins in membranes require that one considers the membrane as a many-particle system whose properties are collectively determined by the assembly and not only by the chemical properties of the individual lipids and proteins [13]. Cooperative phenomena in membranes manifested in terms of differentiated regions or domains, organized in space and time, are a hallmark of a correlated liquid-crystalline fluid [14]. This organization in space and time is a natural and unavoidable consequence of the physical interactions among the different molecules. The challenge is to characterize and measure the characteristic scales of this collective behavior. This is not an easy undertaking, since discernable structuring may only emerge on very small length scales or on very fast time scales. The membrane is a lively and dynamic place.

It has been known for a long time that lipid domains and membrane heterogeneity persist in lipid bilayers and biological membranes [15]. However, the recent raft hypothesis and the subsequent hype have stimulated more researchers from a broader range of disciplines to search for lateral membrane structure and to relate it to function. The raft hypothesis is still rather controversial and a lot of quantitative work needs to be done in order to assess its validity [11].

One thing is clear, however. Considering that functional membranes are two-dimensional liquids and remembering that lateral diffusion is a requirement for many membrane functions, the static picture shown in Fig. 2 cannot be correct or at least it does not give the full picture. It is too static and it overlooks the fact that entropy is a dominant source of the thermodynamic stability. Furthermore, the crucial question remains as to how large and how long-lived such rafts are [11]. Sizes from a few molecules to micrometer size have been suggested. One clue to this question may come from pictures like those in Fig. 3 [8], which shows examples of respectively small domains (nanometer range) in a supported lipid membrane studied by atomic force microscopy and larger domains (micrometer range) in giant unilamellar liposomes studied by fluorescence microscopy. Both images refer to membranes with integral membrane proteins and it is seen that lateral structures may arise on many different length scales.

The physical interactions between the molecules in a lipid membrane determine a so-called persistence (or coherence) length. This length scale is a measure of the effective range over which the interactions operate and lead to structure and fluctuations in structure. The actual value of the persistence length is not only determined by the molecular interactions but it is also dependent on thermodynamic conditions and composition. The persistence length is a measure of the lipid cooperativity (or fluctuations), which in turn is the underlying source of the domain formation. Roughly, the persistence length is the average size of the domains. The range over which different proteins can 'feel' each other through the lipid bilayer is also set by the persistence length [16]. Hence, the small (nanometer) scale structure of membranes is intimately related to lipid–protein interactions. Inspired by the pictures in Figs. 1 and 2, this statement can be rephrased to assert that the extension of the lipid annulus or the size of the lipid raft is proportional to the persistence length. A key question is therefore to determine the persistence length by appropriate physical tools. Its range can vary from a single layer of lipids around the protein to very many. In some sense one can say that the proteins pick up or harvest the lipid fluctuations and domains in the lipid bilayer. This in turn leads to stabilization of the domains. Hence, the lateral organization of proteins in a lipid bilayer can, to some extent, be modulated by altering the persistence length, e.g., by changing temperature or by adding specific substances, such as drugs, that will change the coherence length.

In Section 6, we shall show how atomic-scale Molecular Dynamics simulation techniques can be used to investigate how the persistence length manifests itself in lipid–protein interactions and leads to different quantitative measures of

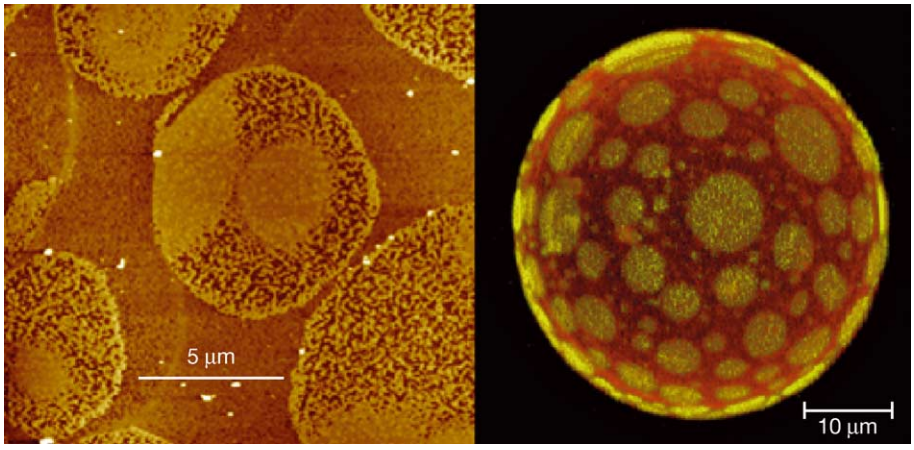

Fig. 3. Lipid domains in native pulmonary surfactant membranes consisting of lipids and proteins. To the left: Atomic force microscopy image of a supported bilayer on mica. Courtesy of Dr. Adam C. Simonsen. To the right: Fluorescence microscopy image of a giant unilamellar liposome. Courtesy of Dr. Luis Bagatolli. Adapted from Ref. [8].

its range and how it depends on various factors, such as the type of lipid.

3. Hydrophobic matching—an ancient mechanism of lipid–protein interactions

All integral membrane proteins have a similar structural motif with a hydrophobic domain, α-helical or β-sheet, that traverses the hydrophobic core of the lipid-bilayer membrane as shown in Fig. 1. The number of membrane-spanning parts of the amino acid sequence ranges from one to more than 12. The hydrophobic domain contains some of the evolutionarily most conserved sequences found in proteins [17]. This suggests that the trans-bilayer coupling between lipids and proteins may be an ancient mechanism that has generic as well as fundamental implications for membrane proteins interactions and hence for biological function.

It has earlier been suggested [18,19] that this coupling is based on a physical principle which dictates that the hydrophobic part of the proteins for energetic reasons has to be matched to the hydrophobic thickness of the lipid-bilayer membrane in which they are imbedded [1,18]. As we shall review in Section 4, there is a substantial amount of experimental evidence that indirectly points to the presence of hydrophobic matching in reconstituted membrane-protein systems and that the degree of matching influences the functioning of membrane channels, pumps, and transporters [20,26], as well as how integral membrane proteins are inserted into, secreted through, and folded within the membrane [21,22].

The physical constraint imposed on integral membrane proteins by the lipid bilayer thickness as illustrated in Fig. 1 suggests that a mechanical hydrophobic matching principle may be operative. Hydrophobic matching means that the hydrophobic length of the trans-membrane domain is matched to the hydrophobic thickness of the lipid bilayer as illustrated in Fig. 4. In order to compensate for the mismatch, the soft lipid bilayer yields and the lipid molecules closest to the protein stretch out or compress in order to cover the hydrophobic core of the protein. This leads to a perturbed region around the protein.

There are obvious energetic advantages of matching. If we for a moment consider a single protein in a membrane and neglect the entropy of mixing of lipids and proteins, the free energy of the system can in the simplest possible theoretical setting be expressed in terms of the mismatch

$$\text{hydrophobic mismatch} = |d_P - d_L| \tag{1}$$

between the lipid-bilayer hydrophobic thickness, d_L, and the protein hydrophobic length, d_P, respectively, as [23,24]

$$G = G^\circ + k\left(\frac{\rho_P}{\pi\xi_L} + 1\right)|d_P - d_L|^2, \tag{2}$$

where G° is the free energy of the unperturbed

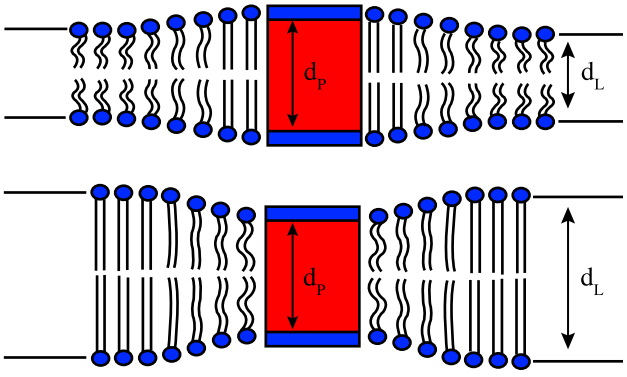

Fig. 4. Schematic illustration of hydrophobic matching of a integral membrane protein that is embedded in a thin (top) and a thick (bottom) membrane. Adapted from Ref. [20].

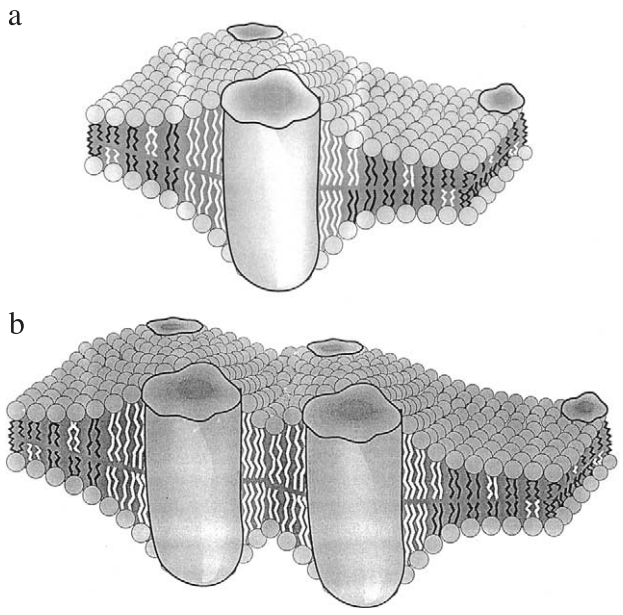

Fig. 5. Schematic illustration of integral membrane proteins embedded in a lipid bilayer that is hydrophobically thinner than the hydrophobic domain of the protein. (a) Hydrophobic matching implies formation of a region of lipids around the protein that conform to the hydrophobic matching condition either by stretching the acyl chains or by recruiting the better matched lipid species at the interface. (b) Hydrophobic matching implies a lipid-mediated mechanism for protein aggregation in the plane of the membrane.

membrane and k is a phenomenological constant related to the bilayer area compressibility modulus. ξ_L is the persistence length of the lipid-bilayer fluctuations described qualitatively in Section 2 and ρ_P is the circumference of the protein which is assumed to have a cylindrical shape. The dependence on protein concentration is implicitly given through the equilibrium bilayer thickness, d_L, which is determined by minimization of the total free energy. Within this theory, the full excess free energy derives from an elastic distortion of the bilayer and this excess free energy is according to Eq. (2) proportional to the square of the hydrophobic mismatch. From this expression, the equilibrium thermodynamics of the lipid–protein can be derived. However, in order to determine the profile of the elastic distortion of the lipids near the protein, a more detailed theory accounting for the local thickness have to be invoked. We shall come back to that in Section 5.

Hydrophobic mismatch and the possibly imposed local curvature stress may therefore be a controlling mechanism for the way proteins interact with lipids in membranes. This mechanism could also be the basis for lipid sorting at the lipid–protein interface as illustrated in Fig. 5a [25] in the case of a membrane that is too thin to accommodate the protein. For a lipid bilayer with a single lipid species, this perturbed interface region in Fig. 5a is characterized by a larger average lipid bilayer thickness and a higher conformational chain order. Since lipid bilayers and membranes under physiological conditions are liquids, the perturbed region is a statistical entity in the sense that lipids diffuse in and out of the region.

It has previously been reviewed how hydrophobic matching provides a physical route to protein organization in membranes [19]. This is illustrated in Fig. 5b in the case of two proteins. In that case, if the distance between the proteins becomes comparable to the persistence length, the annuli of the proteins overlap, which tends to lower the free energy and hence facilitates an effective lipid-mediated attractive protein–protein interaction.

It has been pointed out in the work by Cantor [27] (see also the paper by Cantor in the present issue) that it may not be the hydrophobic thickness that provides the direct mechanic coupling between the lipid bilayer and the protein, but rather some other membrane property which is related to the hydrophobic thickness. The lateral pressure profile shown in Fig. 6 is the most obvious candidate. Due to the anisotropic nature of the membrane, a highly nontrivial trans-bilayer pressure profile is established across the bilayer, reflecting the fact that the high interfacial tensile stress at the water-hydrophobic interface is counteracted by repulsive forces in the head-group region and by the chain pressure in the middle of the membrane. The resulting profile and changes in this profile can lead to conformational changes in the protein as illustrated in Fig. 7, provided the protein has a non-cylindrical shape, e.g., the hourglass form of a helix bundle.

Having established a plausible physical mechanism for lipid–protein interactions, it becomes possible to envisage ways of manipulating membrane proteins and their function by changing the hydrophobic thickness of a membrane or by changing the pressure profile, e.g., by shifting the balance of the pressure between the head-group and acyl-chain part of the bilayer. As reviewed in Ref. [28], a number of drugs may have their action by acting directly on the lipids, changing hydrophobic thickness or pressure profile, and thereby indirectly couple to the protein and its function. This mechanism has been worked out in detail by Cantor [29] in the case of general anesthetics. It has most recently formed the basis for a

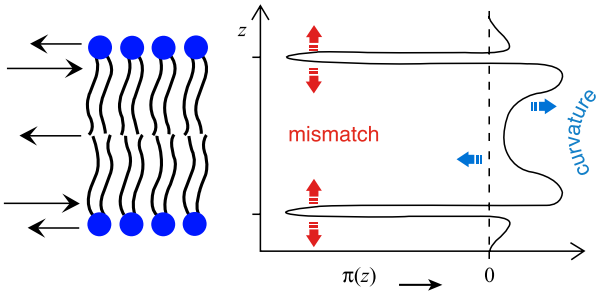

Fig. 6. To the left is shown a lipid bilayer with indication of the forces that act within the layer. To the right is shown the corresponding lateral pressure profile, $\pi(z)$. The effects of hydrophobic mismatch and curvature stress on the profile are indicated. Adapted from Ref. [55].

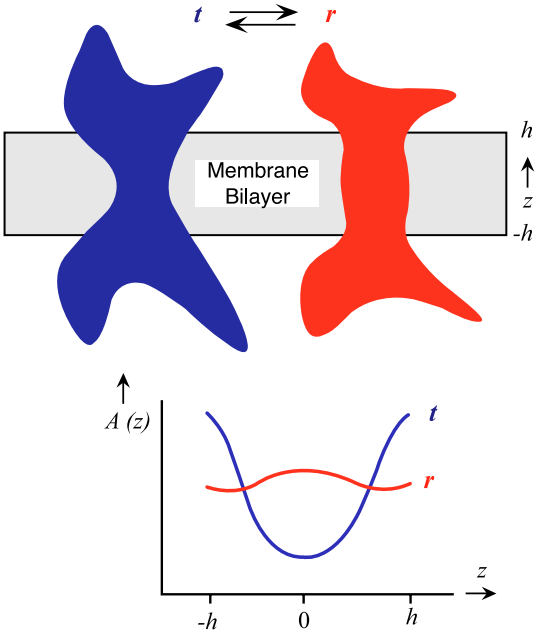

Fig. 7. Schematic illustration of the change in cross-sectional area profile, $A(z)$, of an integral membrane protein that undergoes a conformational transition and a shape change in the lateral pressure profile, $\pi(z)$, of a lipid bilayer. Courtesy of Dr. Robert Cantor.

novel hypothesis for receptor desensitization by neurotransmitters [30]. According to this hypothesis, the rapid, saturable binding of a neurotransmitter to its receptor that results in activation is accompanied by a nonspecific and slower action of the neurotransmitter on the receptor by diffusing into the postsynaptic membrane and thereby changing its physical properties, e.g., the lateral pressure profile. This in turn causes the shift in receptor conformational equilibrium related to receptor desensitization.

4. Experimental evidence for hydrophobic matching in control of protein function

4.1. Synthetic membrane-spanning peptides

The finer details of the hydrophobic matching principle have been studied intensively in model membrane systems with synthetic amphiphilic polypeptides. These peptides, whose molecular structure is known in full detail, can be specifically designed to span the membrane and they can be synthesized with different lengths of the hydrophobic domain in order to vary the mismatch. Examples include gramicidin A and analogues hereof [31,32] as well as the so-called WALP peptides that are α-helical peptides made of a main stretch of alternating hydrophobic Leu and Ala residues of varying length, terminated by Trp residues [33–36]. The effect of hydrophobic matching of the WALP peptides on a wide range of aspects of lipid–protein interactions, including lipid annulus, peptide tilt, peptide aggregation and insertion, as well as peptide structure, has been studied very intensively. However, since the WALP peptides do not support any membrane function per se, they will not be described further in the present paper. The reader is referred to a recent review paper by Killian [33] for an account of these synthetic peptides as models for intrinsic membrane proteins.

In contrast, gramicidin A, although a very simple helical peptide, does support a function as a channel selective to small cations (and water). The activity and life time of the channel can be studied by electrophysiological techniques down to the single-channel level. Gramicidin A in lipid membranes therefore furnishes a particularly elegant and quantitative approach for studying the effect of hydrophobic matching and lipid-induced curvature stress on the opening and closing of membrane channels. Gramicidin A is an antibiotic that forms dimers in lipid membranes by joining two monomers back to back. Only the dimer is conducting. The gramicidin channel can be considered a simple model for the more complex opening and closing of a real membrane channel protein. Obviously, the propensity for forming gramicidin dimers, and hence for activating the model protein, depends on hydrophobic matching and, in the case of a mismatch, on how well the lipids can adopt to a locally curved interface towards the dimer [37,38].

Studies of gramicidin A in membrane systems have not only shown that a good hydrophobic match enhances dimer formation. They have also clearly demonstrated that in the case of a mismatch, where the bilayer is too thick to accommodate the dimer, the formation of dimers can be facilitated by adding lipids which have propensity for forming curved structures, such as cholesterol, lysolipids, and certain drugs [39,40]. These lipids presumably help to mediate the curvature stress that otherwise would build up at the lipid–peptide interface. In thick bilayers, gramicidin A has been found to induce fully developed H_{II} phases. An interesting corollary to these observations is that gramicidin A can be used as a molecular force transducer which can be used to measure the elastic stresses not only in model membranes but also in real biological membranes where it is introduced in very small amounts and where its channel activity is measured by electrophysiological techniques [41].

4.2. Protein function by hydrophobic matching

Except for small and skinny peptides and proteins that traverse the membrane with a single amino acid strand [31,32,34], no direct evidence of the hydrophobic matching principle has yet been demonstrated in molecular detail for any real trans-membrane protein. However, there is a growing body of indirect experimental evidence, some of which was recently reviewed by Dumas at al. [20] and by Lee [26]. It is well known that membrane proteins more often than not exhibit a requirement for specific lipids. In

some cases, it is known that there are chemical factors behind this requirement, e.g., in terms of specific binding. However, in most cases, it is not clear whether the lipid requirement is no more specific than another clever choice of a lipid-membrane composition can equally well support the membrane function. That is, the lipids impart the membrane with a certain emergent property, e.g., curvature stress, lateral pressure profile, domain formation, or possibly hydrophobic thickness, and it may be this emergent or collective property that controls the protein function.

It appears to be a general finding that proteins in their natural membrane are well matched to its hydrophobic thickness, i.e. the thickness of the physiologically relevant liquid membrane phase. Almost all integral membrane proteins stop functioning when the membrane is taken into the solid phase. This makes sense considering that the bilayer thickness is substantially larger in the solid phase. Moreover, in the solid phase, lateral diffusion is slowed down at least two orders of magnitude. This is another important reason why membranes stop functioning when taken into solid phases.

There is a vast amount of experimental evidence which strongly suggests that the hydrophobic matching principle, or some other principle related to that, is relevant for membrane organization as well as for membrane function [20,26]. For example, it has been found for a number of membrane channels, ion pumps, and sugar transporters that they, when incorporated into lipid bilayers of different thickness, function optimally for a certain narrow range of thicknesses, where they presumably are hydrophobically well matched. Thickness alterations induced internally or by external stimuli may therefore be seen as a way of triggering these proteins to enhance or suppress their function as pictured schematically in Fig. 1. To illustrate the principle, we shall describe a couple of examples in more detail.

The first example concerns the 473-amino-acid integral membrane protein melibiose permease which is a cation/sugar symporter from *E. coli*. This protein catalyzes cell accumulation of α-galactosides such as melibiose. Dumas et al. [42] have studied the melibiose transport across lipid membranes of different hydrophobic thickness with the aim of clarifying the relevance of the hydrophobic matching condition for the function of melibiose permease. The resulting data shown in Fig. 8 provide distinct evidence for a strong dependence of transport properties on hydrophobic thickness. The data show clearly that the function of melibiose permease is at an optimum for a particular bilayer thickness.

Another example refers to Fig. 9, which shows that the activity of two different integral membrane proteins that pump ions across membranes depends on the thickness of the membrane. Ca^{2+}-ATPase is important for muscle cell action whereas Na^{+},K^{+}-ATPase takes care of the delicate balance of sodium and potassium ions across membranes. The figure shows that the activity of both ion pumps is

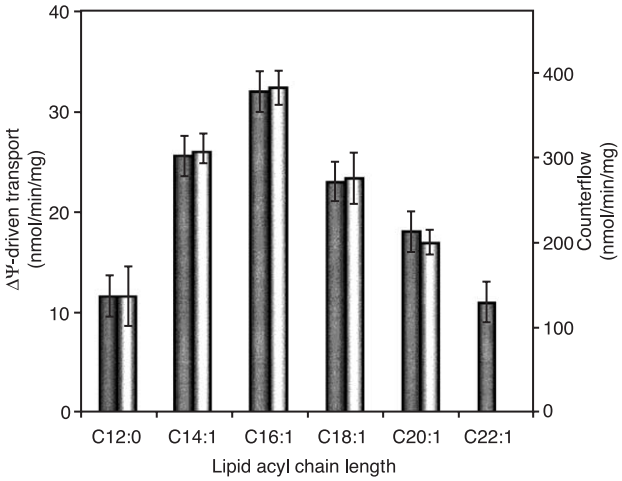

Fig. 8. Melibiose permease-mediated transport (left axis) and corresponding counterflow (right axis) of melibiose through proteo-liposomes made of diacyl phosphatidylcholine lipids of varying acyl chain length. A clear optimum in transport is observed at intermediate chain lengths corresponding to a particular lipid bilayer hydrophobic thickness. Adapted from Ref. [42].

maximal for a certain lipid type and hence for a specific membrane thickness. If cholesterol is added to the membrane, the data in Fig. 9b demonstrate that the maximum moves towards lipid membranes made of shorter lipids. This can be rationalized via the hydrophobic matching principle, recalling that cholesterol tends to thicken fluid membranes, which in turn will compensate for the shorter lipids.

This latter observation suggests a more general principle to be operative by which cholesterol may be used as a regulator of membrane function and in the sorting and targeting of proteins, possibly via hydrophobic matching. The following serves as an illustration. Proteins are synthesized at the ribosomes placed in the endoplasmic reticulum. From there they are transported via the Golgi to the various parts of the cell where they belong, e.g., in the plasma membrane. This transport, which is referred to as the secretory pathway, requires a sorting of the proteins which is performed in the Golgi. Some proteins carry specific tags that will actively target them to their destination, others will passively flow through the cell [44].

The question arises as to how these flowing proteins end up in the right membranes? It has been proposed that the sorting along the secretory pathway may be performed by means of a gradient in the hydrophobic thickness of the membrane systems which the proteins have to pass on their way to their target. Indeed, the membrane contents of cholesterol and sphingomyelin, which both tend to enlarge membrane thickness, are found to increase going from the endoplasmic reticulum, via the Golgi, to the plasma membrane. Furthermore, there is evidence that the proteins, which are supposed to stay in the Golgi, have hydrophobic domains that are shorter by about five amino acids

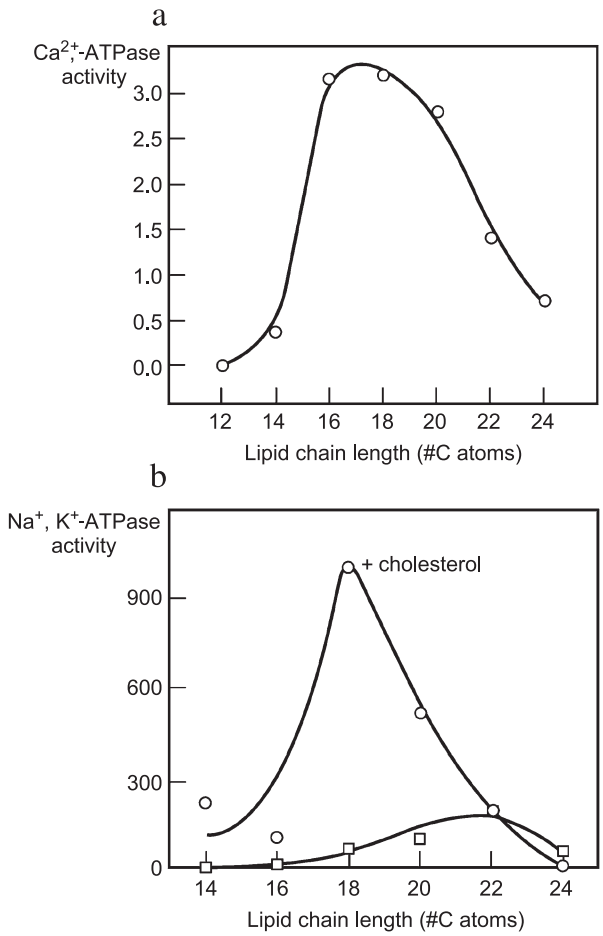

Fig. 9. (a) Activity of the membrane-bound enzyme Ca^{2+}-ATPase as a function of the hydrophobic thickness of the lipid bilayers it is incorporated in. The hydrophobic thickness is given by the number of carbon atoms of mono-unsaturated PC lipids. The activity exhibits a clear maximum. Adapted from Ref. [26]. (b) Activity of the membrane-bound enzyme Na^{+},K^{+}-ATPase as a function of the hydrophobic thickness of the lipid bilayers it is incorporated in. When cholesterol is incorporated in the amount of 40%, the maximum is moved towards membranes made of shorter lipids. Adapted from Ref. [43].

compared to those of the plasma membrane. The set of different membranes along the secretory pathway may hence act as a molecular sieve, exploiting the hydrophobic matching condition. It is possible that this sieving mechanism is controlled by membrane rafts. Since cholesterol has a significant effect on membrane thickness and since integral membrane proteins are hydrophobically matched to their membranes, it is likely that the trans-membrane proteins have closely co-evolved along with the sterols.

4.3. Protein function by lipid-bilayer curvature stress

Hydrophobic matching and bilayer curvature stress are not independent properties as indicated in Fig. 6 [45]. In this section, we shall discuss how curvature stress is involved in the interaction between lipid and proteins, and, for the sake of comparison, we shall describe examples of both peripheral and trans-membrane proteins with reference to Fig. 10. Closer inspection of Figs. 5 and 10 suggests that although membrane surface properties and bilayer hydrophobic matching may be important for the way peripheral and integral membrane proteins interact with membranes, these pictures do not fully appreciate the importance of the built-in curvature stress in the bilayer.

Since lipid molecules have effective shapes, they display propensity for forming non-lamellar phases, and hence contribute to the lateral stress profile of the membrane. The way proteins perturb lipids on the one side, and the way lipids exert stresses on the proteins on the other side would have to involve this feature [27]. This becomes particularly obvious when asking how lipids can influence the functioning of integral membrane proteins or how lipid structure may influence the binding of peripheral proteins.

Although being two sides of the same problem, we shall for convenience first discuss consequences of non-lamellar lipids on lipid–protein interactions and then describe how the lateral pressure profile relates to protein function.

A substantial part of the lipids found in natural membranes, e.g., PE lipids, are very poor bilayer formers and in fact have propensity for non-lamellar structures like the inverted hexagonal phase, H_{II}. This intrinsic instability towards curved structures must have some advantage for function [46–49]. One could imagine the instability to be

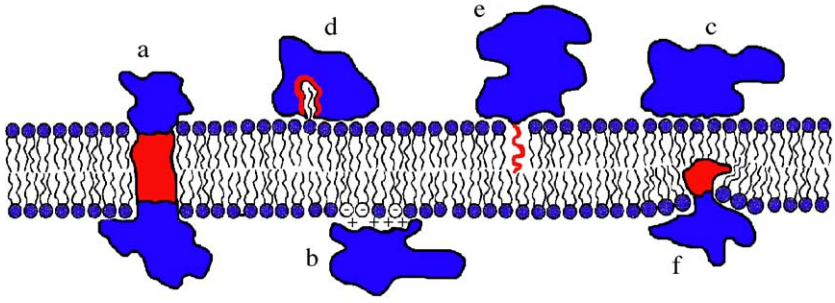

Fig. 10. Schematic illustration of integral membrane proteins that spans the bilayer (a), compared to five modes of binding a peripheral protein to a membrane surface: (b) electrostatic binding; (c) nonspecific binding by weak physical forces; (d) anchoring via a lipid extended conformation; (e) anchoring by an acyl-chain anchor attached to the protein; (f) amphiphilic protein partially penetrating the bilayer.

locally released in connection with protein binding, protein insertion, membrane fusion, and conformational changes in the cycle of protein functions.

Let us start with a peripheral membrane protein in order to see how this could work. Protein kinase C is one of the most important enzymes that is involved in the signal transduction system of the cell. Upon stimulation of the cell by, e.g., neurotransmitters, hormones, and growth factors, protein kinase C becomes activated upon binding to the plasma membrane, leading to a complicated cascade of biochemical signals that eventually influence cell growth, cell differentiation, as well as exocytosis. A requirement for binding to the membrane and hence for activation of the enzyme is lipids with acidic head groups, like phosphatidylserine, and the presence of calcium ions. Calcium ions require water for solvation, and in the competition for water, the membrane surface becomes dehydrated leading to a larger curvature stress [50].

It has been proposed by Kinnunen [47] that this curvature stress could be released if some lipid molecules assume an extended chain conformation by flipping one of the acyl chains to the outside of the membrane. This flip would normally be energetically very costly because of the hydrophobic effect. However, if the chain can be accommodated in a putative hydrophobic crevice in a protein as illustrated in Fig. 10d, it will not only release the curvature stress of the membrane but at the same time also facilitate the membrane anchoring and hence the activation of the enzyme. Protein kinase C has such a hydrophobic crevice. The presence of the extended chain anchorage is further supported by the finding that the addition of PE lipids enhances the enzyme activity. PE lipids have a small head group and hence display propensity for forming H_{II} phases. This further increases the curvature stress and promotes the formation of the extended lipid chain conformation, which in turn explains the enhanced activation of protein kinase C. There are also some indications that the mechanism of anchoring via a lipid extended conformation may play a role for binding of cytochrome *c* [51] as well as number of other membrane active proteins that indeed have hydrophobic pockets to accommodate the extended lipid chain.

We then turn to the integral membrane protein rhodopsin which is a seven-helix trans-membrane protein. Rhodopsin is the light-sensitive protein in the visual pigment of our retina which, upon activation with light, initiates the signaling pathway that eventually leads to vision. An essential stage of this process involves a certain transition between two conformational states of rhodopsin, the so-called M-I and M-II states. The M-II state is believed to correspond to a more elongated form of rhodopsin than the M-I state. The transition therefore implies a change in hydrophobic mismatch. Studies have shown that the M-II state requires the presence of lipids that have propensity for forming H_{II} phases [52]. The retinal rod outer segment membranes, in which rhodopsin exhibits its function, are known to have almost 50% of the polyunsaturated fatty acid docosahexaenoic acid (DHA), which, due to the many double bonds, indeed supports curved structures. The fact that the M-I to M-II transition can be fully activated by other non-lamellar forming lipids, like phospholipids with PE head groups [52], suggests that it is the physical curvature stress release by the lipids rather than a specific chemical reaction between DHA and rhodopsin which is the controlling mechanism. Additional support for this viewpoint is the finding that short alcohol molecules, which by are known to position themselves in the hydrophobic–hydrophilic interface of the membrane and hence counteract the stability of the H_{II} phase, can deactivate the transition [53].

Robert Cantor has put the relationship between curvature stress and protein function on a more quantitative footing by presenting a simple mechanistic model picture based on how the lateral pressure profile $\pi(z)$, cf. Fig. 6, can couple to protein function via the stresses it exerts on a trans-membrane protein [45] as illustrated in Fig. 7. This picture relates the work, W, required to induce a transition between two states r and t of the protein, characterized by two different cross-sectional area profiles $A_r(z)$ and $A_t(z)$ of the protein, to the lateral pressure profile, $\pi(z)$,

$$W = -\int_z \pi(z)[A_t(z) - A_r(z)]\ \mathrm{d}z. \tag{3}$$

The crucial point here is that the protein needs to have a non-cylindrical shape in order to sense the lateral pressure profile and the possible changes in the profile under the influence of other factors. Estimates of the amount of work, W, required to change the conformational state of an integral membrane protein suggest that the stress changes which the lipid bilayer can provide indeed should suffice to activate the protein [45].

It might be expected that many integral membrane proteins are rather rigid and only little influenced by the strain from the membrane they are imbedded in. However, as we shall see in the case of an aquaporin as described in Section 6, even this large and fairly solid channel is susceptible to the forces exerted by the lipids. There is, however, a particular class of membrane proteins, the mechanosensitive channels, that have evolved to facilitate ion conductance in response to a stress exerted by the membrane [54,55]. These proteins are nano-machines that work as transducers of mechanical strain dissipated from the membrane. The most well-studied example is the bacterial large conductance mechanosensitive channel (MscL) from *E. coli* shown in Fig. 11. Hydrophobic matching and curvature stress concepts have been used to interpret the experimental data for the conductance and how it varies when non-lamellar lipid species are incorporated into the membrane [55]. MscL is a helix bundle protein and experiments as well as Molecular Dynamics simulations

have supported a mechanism for channel opening that involves an iris-like expansion of the conducting pore [56,57]. The illustrations in Fig. 11 show the channel and how the opening of the channel can be simulated by steered Molecular Dynamics techniques [56,57].

4.4. Insertion of peptides and proteins into lipid bilayers controlled by hydrophobic matching

It is an outstanding problem in molecular cell biology how proteins along the secretory pathway get selected for certain organelles and membrane types [58]. It has been proposed that membrane thickness and hydrophobic matching may be part of the selection mechanism [44]: the proteins end up in the membrane that provides for the best hydrophobic matching.

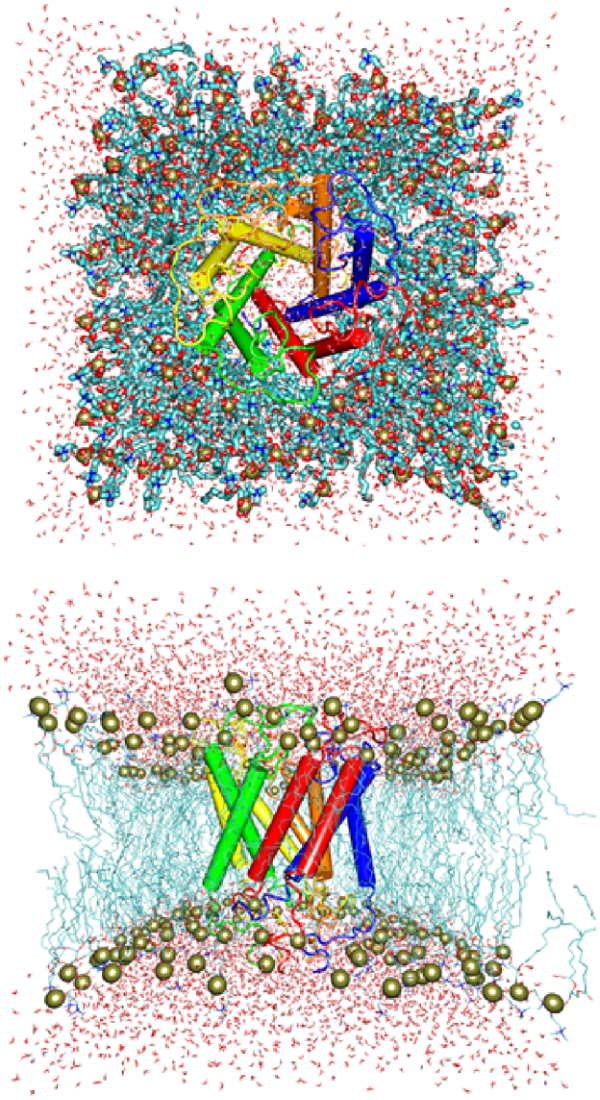

Fig. 11. Molecular Dynamics simulation snapshots of the bacterial large conductance mechanosensitive channel (MscL) from *E. coli*. Top and side views are shown corresponding to the beginning of the simulation where lateral tension is exerted on the channel. The system comprises 242 lipids and 16,148 water molecules; in total, 88,097 atoms. Courtesy of Dr. Klaus Schulten. Reprinted with permission from the Theoretical and Computational Biophysics Group at University of Illinois at Urbana–Champaign and adapted from Ref. [56].

A couple of recent studies have investigated the importance of hydrophobic matching for insertion and folding of integral membrane proteins into lipid bilayers of different thickness. Ridder et al. [21] found for the Pf3 coat protein of *E. coli*, which has a single membrane spanning domain, that the insertion was most efficient under hydrophobic matching conditions.

Hong and Tamm [22] recently succeeded in designing a complete reversible assay using denaturants for studying the thermodynamics of insertion and folding of the outer membrane protein OmpA from *E. coli*. This protein folds into lipid bilayers as an eight-stranded β-barrel structure of the N-terminal trans-membrane domain. The assay permitted a study of the folding–unfolding equilibria and the folding pathways as a function of lipid bilayer hydrophobic thickness. The situation is illustrated in Fig. 12. It was found that the degree of hydrophobic matching is a major determinant of both the folding and the insertion process. For thin membranes, an intermediate state was found in which the protein is inserted but not folded. Moreover, the distribution of the lateral stresses in the bilayer was asserted to be important since the hourglass-shaped OmpA protein is stabilized by a relatively large lateral pressure in the chain region (see Fig. 12). It was concluded that the bilayer elastic forces contribute to the thermodynamic stability of OmpA, and Hong and Tamm [22] surmised that this may be true of most integral membrane proteins.

5. Theory of lipid–protein interactions

The theory of lipid–protein interactions formulated in terms of hydrophobic matching has been reviewed in Ref. [24]. For the benefit of the discussion in Section 6, we shall here derive an expression for the lipid (thickness) order profile around a protein in the simplest possible setting. The expression for this profile provides a formula for extracting the coherence or persistence length of lipid–protein interactions as mentioned in Section 2. More elaborate theories are described in Refs. [59–61] in the context of gramicidin A where more details in the hydrophobic boundary conditions are considered.

We restrict ourselves to a theoretical description including a single order parameter, being the local hydrophobic membrane thickness, $d_L(r)$, resolved as a function of radial distance r from the protein. This theory is a Landau–de Gennes type theory and it provides us with predictions for $d_L(r)$ in two major cases: (I) the case of a relaxed (unconstrained) boundary condition and (II) a constrained boundary condition (see below). In the following, $d_L=d_L(r\rightarrow\infty)$ is the hydrophobic thickness of the unper-

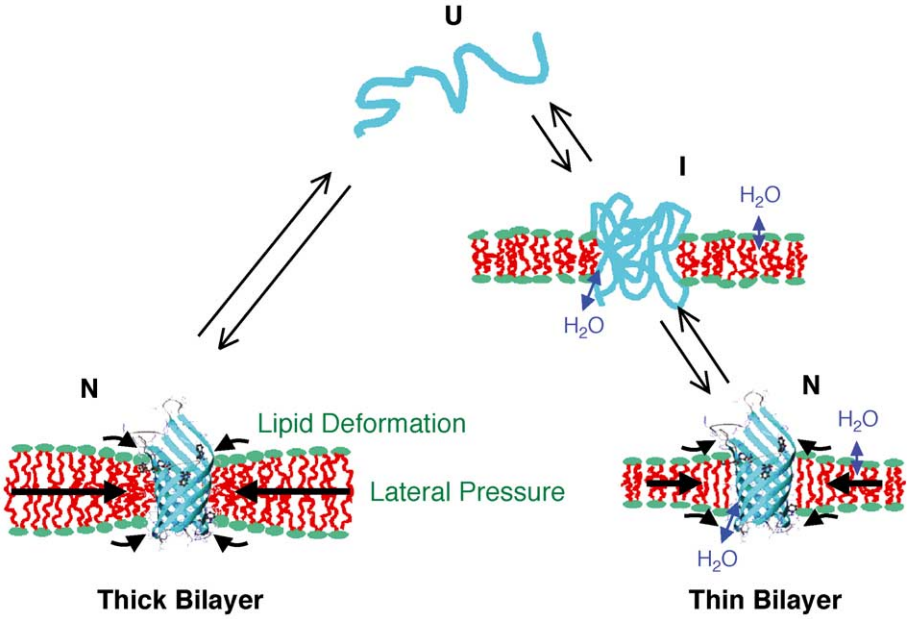

Fig. 12. Illustration of the equilibria between unfolded and folded states of outer membrane protein A (OmpA) of Gram-negative bacteria. OmpA forms a eight-stranded β-barrel in the N-terminal transmembrane domain. Denatured OmpA in the aqueous phase spontaneously refolds into lipid membranes upon removal of the denaturants. The degree of hydrophobic matching is a major determinant of the folding-unfolding equilibria and the folding pathways. In the case of thin membranes, an intermediate state (I) is found in which the protein is inserted but not correctly folded. Adapted from Ref. [22].

turbed lipid bilayer far from the protein, and d_P is the thickness of the hydrophobic core of the protein.

Within Landau–de Gennes theory, the free energy is determined by minimization of the functional integral

$$G = \int \mathrm{d}^d r\, g\left[d_L(r), d_L'(r)\right] \tag{4}$$

where $\mathrm{d}^d r$ is a d-dimensional volume element, $d_L'(r) \equiv \mathrm{d}d_L(r)/\mathrm{d}r$ and $g[d_L(r), d_L'(r)]$ is a local free energy density determined by

$$\frac{\partial g[d_L(r), d_L'(r)]}{\partial d_L(r)} - \frac{\mathrm{d}}{\mathrm{d}r}\left(\frac{\partial g[d_L(r), d_L'(r)]}{\partial d_L'(r)}\right) = 0. \tag{5}$$

(I) *Relaxed boundary condition: $d_L(r=0)=d_P$ and no constraint on the shape $d_L'(r)$.* The free energy density is considered within a Gaussian approximation, i.e., an elastic (harmonic) deformation and a local thickness fluctuation contribute to $g[d(r), d'(r)]$

$$g_I[d_L(r), d_L'(r)] = \frac{a}{2!}[d_L(r) - d_L^\circ]^2 + \frac{c}{2}[d_L'(r)]^2. \tag{6}$$

Inserting Eq. (6) into Eq. (5), the minimum in $g_I[d_L(r), d_L'(r)]$ is obtained for an exponential shape of $d_L(r)$

$$d_L(r) = d_P - (d_L^\circ - d_P)\exp(-r/\xi_P), \quad \xi_P = \sqrt{\frac{a}{c}}, \tag{7}$$

where ξ_P is a deformation coherence length for the profile. ξ_P is proportional to the lipid persistence length, ξ_L, described in Section 3, and the spring constants a and c can be related to k in Eq. (2).

(II) *Constrained boundary condition: $d_L(r=0)=d_P$, and $d_L'(r)\to 0$ for $r\to(\infty, 0)$.* In order to accommodate the constrained boundary condition, one goes beyond a second-order approximation to $g[d_L(r), d_L'(r)]$, thus allowing for higher-order deformation terms in $d_L(r)$

$$g_{II}[d_L(r), d_L'(r)] = \frac{c}{2}[d'(r)]^2 + \frac{a}{2}[d_L(r) - \bar{d}_L]^2 + \frac{b}{4!}[d_L(r) - \bar{d}_L]^4 \tag{8}$$

where $\bar{d}_L \equiv \frac{1}{2}(d_L^\circ + d_P)$. By inserting Eq. (8) into Eq. (5), the minimum is now obtained for a hyperbolic shape, i.e., the so-called 'kink' solution recognized from conventional Cahn–Hilliard theory

$$d_L(r) = d_P + \frac{1}{2}(d_L^\circ - d_P)\tanh\left(\frac{r}{\xi_P}\right), \qquad \xi_P = \sqrt{\frac{a}{c}}. \tag{9}$$

It should be remarked that the constrained boundary condition is somewhat unphysical since it assumes that the inflection point of the hyperbolic tangent is far away from the protein. This will not be the case in reality, where the inflection point will be less than a coherence length displaced from the lipid–protein interface. To remedy this artefact, a more elaborate calculation is needed and it is no longer possible to obtain an analytical expression for the

profile [59]. For the present purpose, the expression in Eq. (9) is good enough to serve as an approximation.

6. Lipids influence the functioning of the glycerol/water channel protein GlpF: a case study [62]

We now describe a case study of an integral membrane protein, GlpF, which is an aquaporin [63], i.e., a water-transporting protein that also facilitates stereoselective trans-membrane transport of glycerol across the plasma membrane of *E. coli* [64]. The protein is a homo-tetramer where each monomer basically is a rigid pore, as shown in Fig. 13. Along with water, each pore allows linear carbohydrate molecules to pass the latter in a stereo-selective fashion, ensured by a particular selectivity filter [64–69] while the water selectivity is maintained by orientational and electrostatic tuning of the pore interior [70–73].

The interaction of GlpF with lipid bilayers has been studied in some detail recently by Molecular Dynamics techniques [62,65,66]. These calculations have provided the first direct and detailed evidence for hydrophobic matching in lipid bilayers incorporated with a large trans-membrane protein [62]. An account of the modelling of GlpF as a glycerol/water channel and as a pure water channel embedded in POPE hydrated bilayers, together with a detailed description of selectivity and transport mechanism, can be found in Refs. [65,66,70,71]. From these studies, a POPE lipid bilayer proved to be a good approximation for the native *E. coli* membrane, reflecting that the bacterial membrane is rich in POPE.

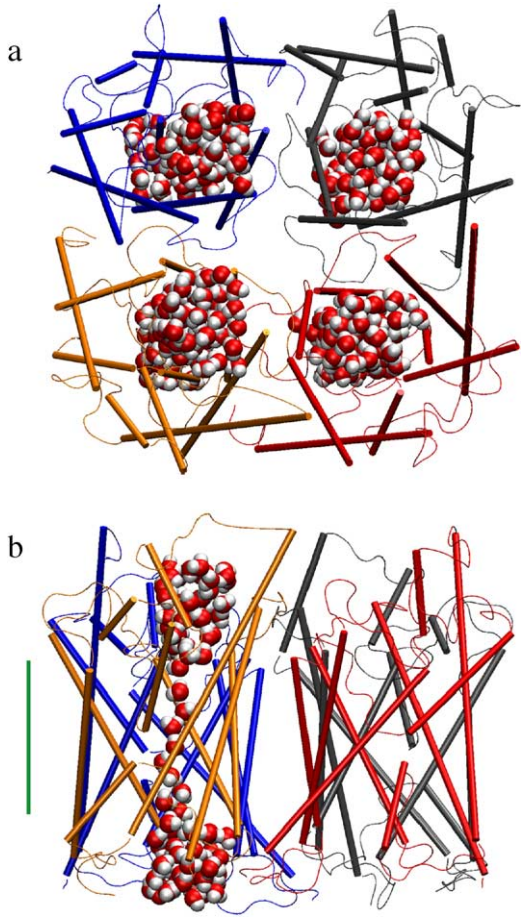

Fig. 13. Snapshot of the glycerol/water channel protein GlpF taken from our Molecular Dynamics simulations of GlpF/POPC. (a) Top view exposing the four water filled trans-membrane pores. (b) Side view showing water crossing one monomer in single file through the constriction region, which is marked by a green bar (b). For the sake of clarity, the water molecules and the lipid bilayer are omitted in (a) and (b).

Below we consider GlpF as a pure water channel and we focus on how the presence of the protein influences the lipids on the one side and how the lipids may possibly influence the structure and function of the protein on the other side. In order to investigate the possible influence of the type of lipid membrane, the channel is here studied both in a POPE bilayer and a POPC bilayer as outlined below.

6.1. Molecular Dynamics techniques

As controls, two different lipid bilayers of 480 fully hydrated POPE and POPC molecules, respectively, were simulated. The pure bilayers were set up for the simulations as follows. First, a crystalline POPE bilayer was generated with the lipid molecules arranged in a regular hexagonal lattice in a periodic rectangular box with dimensions of $122.0\times112.7\times77.0$ Å^3. The membrane was hydrated with 16227 water molecules using Solvate [74] ensuring a hydration of 33 water molecules per POPE molecule. In a subsequent preparation of the hydrated POPC bilayer, the amine hydrogen atoms in the ethanolamine head groups of the POPE bilayers were simply replaced by methyl groups leaving lattice and hydration parameters identical to those of the POPE bilayer. The resulting systems included in total 108.681 atoms (POPE) and 112.999 atoms (POPC).

The GlpF/POPE system reported here, with GlpF acting as a pure water channel, is identical to that in Refs. [70,71]. For setting up the GlpF/POPC system, we made similar lipid headgroup substitutions as done for the pure bilayers above, leaving all other parameters invariant. With 317 lipid molecules present, the original GlpF/POPE system counted in total 106.245 atoms [71,70] while GlpF/POPC counted 109.042 atoms in total.

The MD simulations were performed with NAMD [75] using the CHARMM 27 parameter set [76,77]. The protein/lipid systems were initially minimized and equilibrated in the NPT ensemble, i.e., at constant temperature ($T=310$ K) and pressure ($P=1$ atm) for 100 ps (GlpF/POPE) and 250 ps (GlpF/POPC) with the protein fixed. The protein was subsequently released and the full systems were energy minimized prior to NPT simulations conducted subsequently for 5 ns with T and P again specified as above. Full periodic boundary conditions were imposed in all simulations and the Particle Mesh Ewald method [78] was used for computation of electrostatic forces. For additional

details of the simulation protocol, we refer to Refs. [65,70,71]. Similarly, the pure hydrated POPE and POPC bilayers were initially minimized and simulated for 5 ns in the NPT ensemble using a simulation protocol identical to that of the combined protein/lipid systems. Trajectories were analyzed using VMD [79].

6.2. Direct observation of hydrophobic matching

In Fig. 14 are shown snapshots obtained from the simulations of the two systems after 5 ns simulation time. Representations with (Fig. 14a,c) and without (Fig. 14b,d) the water molecules are shown. It is clearly seen that both the POPE and the POPC bilayers are slightly thinner in vicinity of GlpF and that the lipid chains near the protein contract in order to fulfill the hydrophobic matching condition. This is the first part of our direct evidence of hydrophobic matching in membranes. It should be remarked that the fact that the matching is visible from such snapshots is by far nontrivial. Since the lipid bilayer is in the fluid phase, it is subject to a number of different fast dynamical modes, one of which is single-molecule lipid protrusions out of the membrane surface. These protrusions are very frequent with a typical duration of 10 ps and a coherence length of 2–5 Å normal to the membrane [80]. It should be noted that within the time scale of the simulation, the lateral diffusion of the lipid molecules has only had a minor effect on the organization of the membrane. Qualitatively, similar hydrophobic matching has also been observed in Molecular Dynamics simulations of the mechanosensitive channel MscL and for the chloride conducting channel ClC [56,81].

6.3. Bilayer thickness profiles

The simulated bilayer thickness as a function of time is, in selected radial distances from the protein, shown in Figs. 15a,b and 16a,b for POPE and POPC, respectively. The value for $d_L(r)$ is calculated as the circularly averaged distance between the two opposing hydrophobic/hydrophilic interfaces defined either by the positions of the carbonyl C=O groups ($d_L(r)^{C=O-C=O}$) or the positions of the phosphorus atoms ($d_L(r)^{P-P}$) where the first measure is most appropriate in relation to our hydrophobic matching discussions.

The results of a quantitative analysis of the radial thickness profile, $d_L(r)$, for the bilayer thickness as a function of the distance, r, from the protein/lipid interface are shown in Figs. 15c,d and 16c,d, while numerical values for the relevant structural parameters obtained by fitting $d_L(r)$ to the functional forms in Eqs. (7) and (9) are collected in Table 1. For both the POPE and the POPC bilayer, a well-defined profile is found for both thickness measures. The profiles reflect a smooth thinning of the bilayer going from the unperturbed bilayer towards the protein. At the very interface, the hydrophobic bilayer thickness is closely matched to the thickness of the hydrophobic core of the protein.

Comparison of the thickness profiles for the POPE and POPC bilayers indicates that they have slightly different

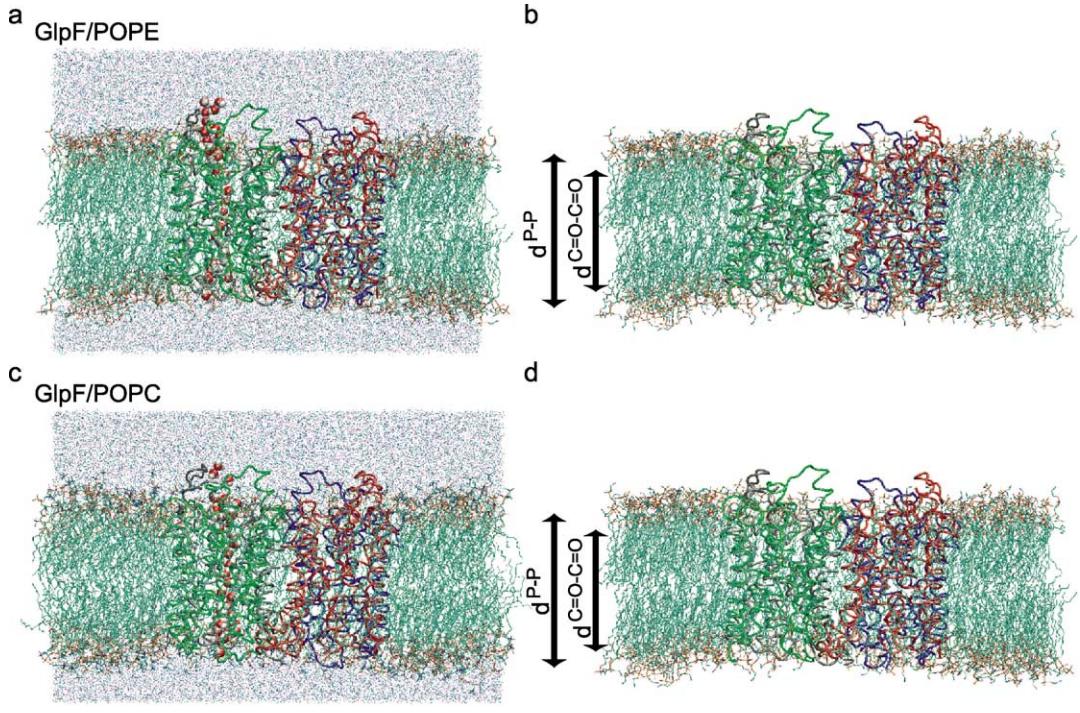

Fig. 14. Snapshots taken after 5 ns of Molecular Dynamics simulations performed using the NAMD program at constant temperature (310 K) and pressure (1 atm) of a GlpF/POPE membrane system (a, b) and a GlpF/POPC membrane system (b, c). Each system contains about 106.000 atoms and the configurations are shown both with water in one monomer (a, c) and without the water molecules and the lipid bilayer (b, d). Bilayer thickness measures d_L^{P-P} and $d_L^{C=O-C=O}$ are indicated by arrows next to panels (b, d).

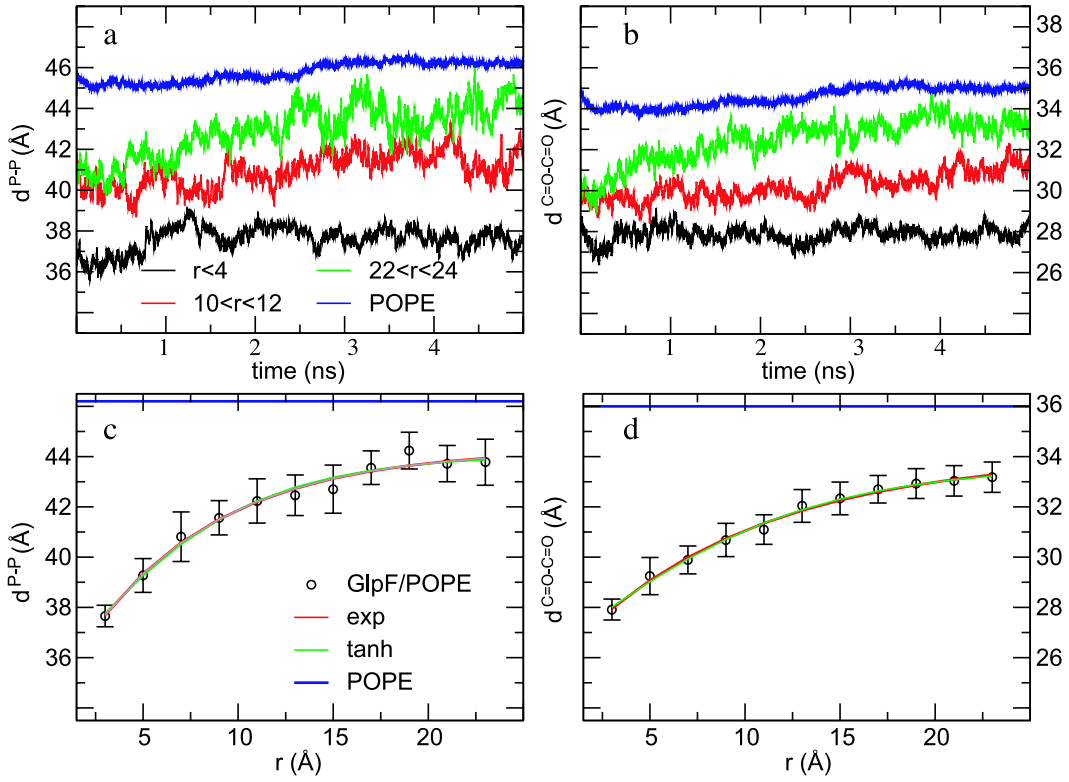

Fig. 15. Bilayer thickness as a function of time (a, b) and radially resolved average bilayer thickness (c, d) for GlpF/POPE. The profiles are calculated as average P–P (a, c) and C=O–C=O (b, d) separations between the monolayers as a function of radial distance from the protein. The bilayer deformation profiles provide a correlation length (ξ_P) as set by the degree of lipid–protein mismatch. Using Landau-de Gennes theory, minimization of the free energy density $G=\int d^2r g[r, d_L(r)]$ we recover, e.g., the hydrophobic (C=O–C=O) thickness of the protein (d_P) and of the pure bilayer (d_L°) in the limit of $r\rightarrow 0$ and $r\rightarrow\infty$, respectively. The bilayer deformation profile in the GlpF/POPE system obeys the functional forms $d_L(r)=d_P-(d_L-d_P)\exp(-r/\xi_P)$ and $d_L(r)=d_P+(1/2)(d_L^\circ-d_P)\tanh(r/\xi_P)$.

shapes and that the relaxation away from the protein is most smooth in GlpF/POPE. By fitting $d_L(r)$ to the two shapes predicted from the theoretical calculations above, cf. Eqs. (7) and (9), we find as listed in Table 1 that the exponential profile and the hyperbolic profile provide essentially equally good fits to GlpF/POPE (cf. RMS errors in Table 1), whereas the fit to the hyperbolic profile (Eq. (9)) is significantly better in the case of GlpF/POPC when considering the hydrophobic measure $d_L^{C=O-C=O}$. According to these fits, the hydrophobic thickness of the protein d_P is about 26 Å for GlpF/POPE and about 24 Å for GlpF/POPC, i.e., essentially identical and very similar to estimates for d_P for other trans-membrane pores proposed from related studies [82]. The equilibrium thickness of the bilayer is approached asymptotically but not fully recovered for both systems, i.e., $d_L(r\rightarrow\infty)<d_L^\circ$, which probably is due to the finite size of the systems.

Furthermore, from these fits, the value of the persistence length, ξ_P, of lipid–protein interactions can be found. We recall that ξ_P is proportional to ξ_L. The values determined for ξ_P in the two cases are rather similar, about 10 Å in general, and indicate that GlpF at 310 K perturbs fluid lipid bilayers over a range corresponding to a few lipid molecular diameters, i.e. typically 40–80 lipid molecules are significantly perturbed. This is the so-called lipid annulus, which is a statistical entity reflecting the fact that the lipids are not bound to the protein but undergo diffusional modes that over time will bring them in and out of the annulus. Moreover, for $r\rightarrow 0$ fewer lipid molecules contribute to the $d_L(r)$ implying that statistical uncertainties are the largest closest to the protein although this effect could be masked by variations (with r) in out-of-plane lipid protrusions.

The nature of the boundary condition at the lipid–protein interface has been investigated intensively in the work by Nielsen and Andersen [61], in particular in relation to the shape of the lipid molecules. Results from analysis of lipid bilayers with gramicidin A have suggested, in accordance with the finding reported above, that PE lipids, due to their smaller head group, conform with the free boundary condition whereas the PC lipids conform with the fixed boundary condition [39,83]. However, the results for the Molecular Dynamics simulations are not conclusive and in any case the difference is very small. Moreover, it should be expected that the details of the boundary condition depend not only on the shape of the lipid molecules but also on the shape of the protein. Obviously, whereas gramicidin A is well approximated by a cylindrical shape, GlpF has a more complex three-dimensional shape not unlike that of an hourglass.

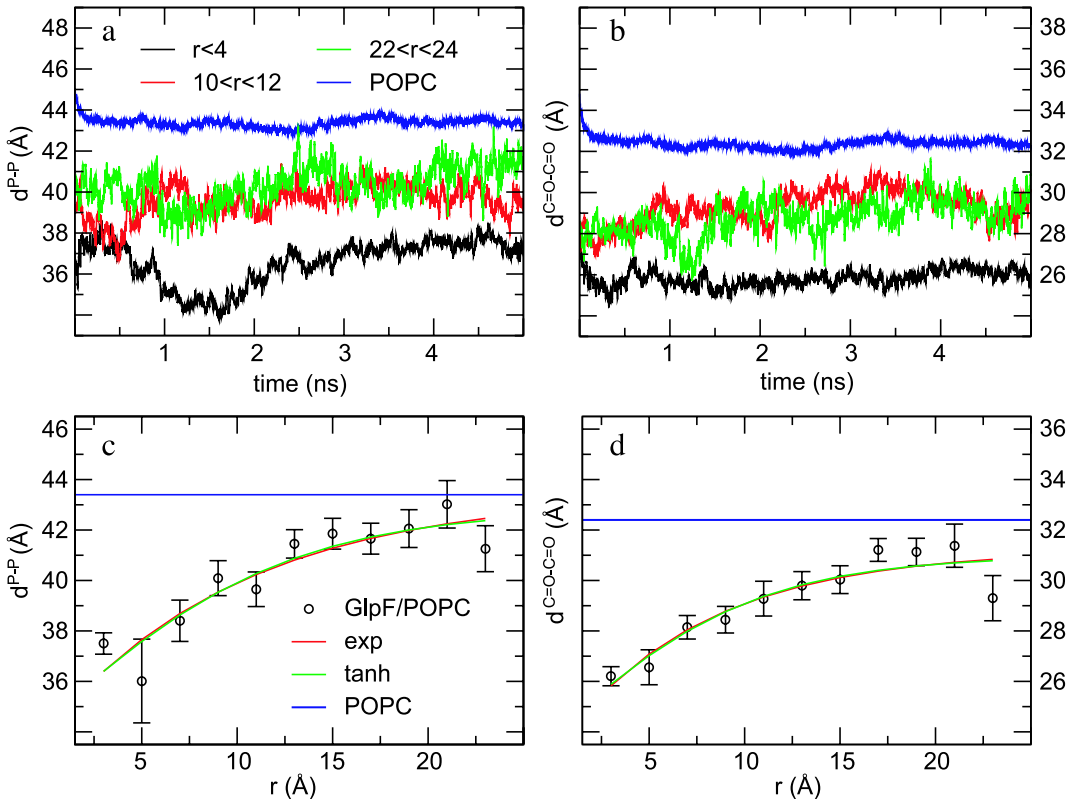

Fig. 16. Bilayer thickness as a function of time (upper panels) and radially resolved average bilayer thickness (lower panels) for GlpF/POPC. Due to the greater mismatch relative to GlpF/POPE, the deformation profile for GlpF/POPC differs next to the protein. The deformation obeys again the functional forms $d_L(r)=d_P-(d_L-d_P)\exp(-r/\xi_P)$ and $d_L(r)=d_P+(1/2)(d_L^\circ-d_P)\tanh(r/\xi_P)$; see Table 1. From least squares fits, ξ_P, d_P and d_L are recovered.

6.4. Lipid acyl-chain order parameter profiles

The degree of chain order along each of the two acyl chains (α=16:0, 18:1c9) of the lipid molecules is conveniently measured by the segmental order parameter

$$S_i^\alpha = \left\langle \frac{1}{2}(3\cos^2\theta_i - 1) \right\rangle, \qquad (10)$$

where θ_i is the angle between the bilayer normal and the normal to the plane spanned by the ith CH_2-group. S_i^α can be measured by nuclear magnetic resonance techniques [84]. It is usually the average value of S_i^α along the chain, the so-called order parameter, which is most readily measured spectroscopically. Deviations of this order parameter in a lipid–protein system relative to the order parameter of a pure lipid membrane can be taken as an indication of the effect of lipid–protein interactions. Due to the intrinsic time scale of the spectroscopic techniques and the fact that the lipid molecules diffuse rapidly in a fluid lipid membrane, it is usually not possible to resolve the spectra in terms of a variation of the order parameter around the protein. This problem does not exist in the Molecular Dynamics approach. In Figs. 17 and 18 are shown order parameter profiles for the 16:0 and 18:1c9 lipid acyl chains resolved with radial distances r to the protein for GlpF/POPE and for GlpF/POPC.

In Fig. 17a,b data for selected radii are shown ($r<4$ Å, $r>25$ Å), indicating in the upper part of the aliphatic chains a consistently increased order in GlpF/POPE relative to the order in pure POPE membranes, whereas in the lower half of

Table 1
Hydrophobic matching quantified

Measure	POPE				POPC			
	Eq. (7)		Eq. (9)		Eq. (7)		Eq. (9)	
	d_L^{P-P}	$d_L^{C=O-C=O}$	d_L^{P-P}	$d_L^{C=O-C=O}$	d_L^{P-P}	$d_L^{C=O-C=O}$	d_L^{P-P}	$d_L^{C=O-C=O}$
d_L(Å)	44.3	34.1	42.9	40.9	52.9	39.2	51.2	38.0
d_P(Å)	34.1	25.8	35.3	26.4	43.4	31.2	34.5	24.0
ξ_P(Å)	7.0	9.9	10.2	13.1	10.2	7.6	12.8	10.8
RMS (10^{-2})	0.6	0.4	0.6	0.4	2.1	2.1	2.1	0.5

Least squares fits to $d_L(r)=d_P-(d_L-d_P)\exp(-r/\xi_P)$ (Eq. (7)) and $d_L^\circ(r)=d_P+(1/2)(d_L^\circ-d_P)\tanh(r/\xi_P)$ (Eq. (9)).

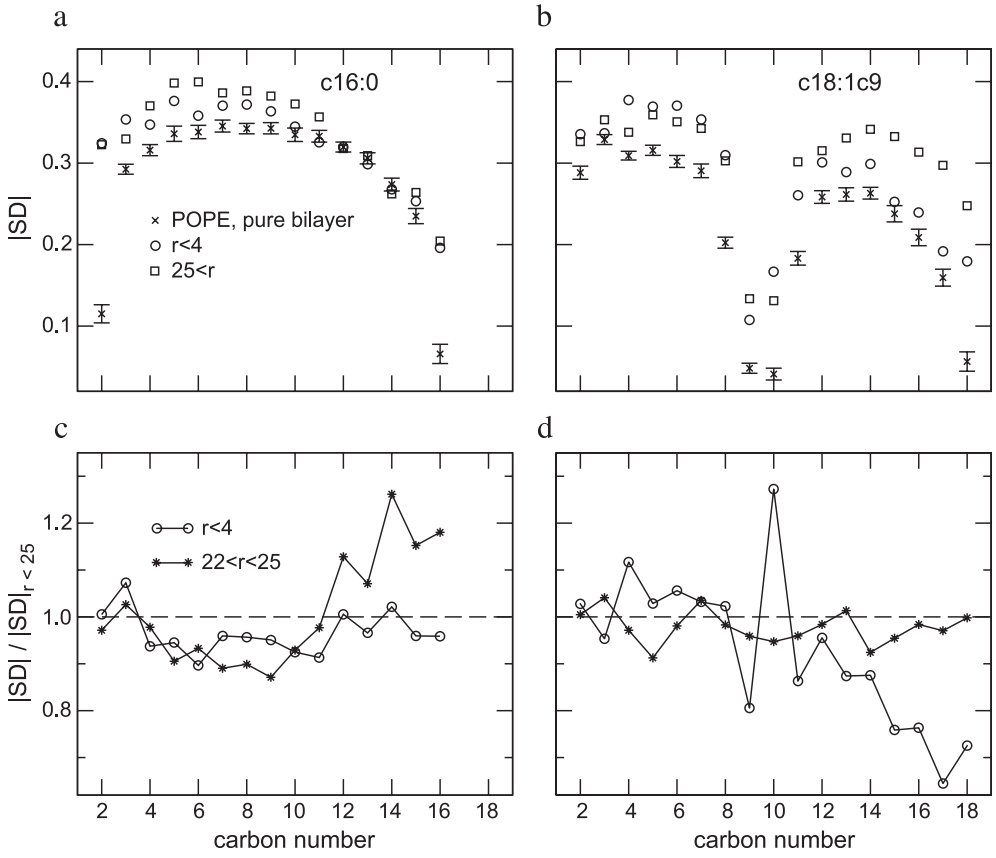

Fig. 17. (a,b) Radially resolved lipid order parameter profiles for GlpF/POPE for the 16:0 and 18:1c9 lipid acyl chains in selected (r<4 Å, r>25 Å) radial distances from the protein. (c, d) Selected (r<4 Å, 22 Å<r<25 Å) GlpF/POPE order parameter profiles in (a, b) normalized by the appropriate r>25 Å data from (a, b).

the 16:0 chain we find similar order as in the pure bilayer (Fig. 17a), i.e., in order to accommodate hydrophobic matching, the 18:1c9 chain undergoes the largest structural changes.

In Fig. 17c,d we show selected (r<4 Å, 22 Å<r<25 Å) GlpF/POPE order parameter profiles normalized by the r>25 Å data in (a,b). The normalization of the 16:0 (r<4 Å) data implies that the order lies close to unity for all CH_2-groups, and is therefore essentially the same in the proximity to the protein as most distant from the protein. For 16:0 (22 Å<r<25 Å) we find more order than most distant from the protein, a finding that (in part) might be related to the finite size of the system. The 18:1c9 (r<4 Å) data show significantly reduced static order in proximity to the protein, i.e., the 18:1c9 chain bends and/or tilts, while satisfying hydrophobic matching at the protein interface, whereas the 18:1c9 (22 Å<r<25 Å) data lies close to the unity line implying the same degree of order as most distant to the protein.

Corresponding results for GlpF/POPC Fig. 18a,b again indicate more order in the GlpF/POPC system than what is found from simulations of a pure POPC bilayer. This applies to both the 16:0 and the 18:1c9 chains. Normalizing the GlpF/POPC profiles by the r>25 Å data, we observe in the tail region increased disorder in the proximity (16:0 (r<4 Å)) of the protein and slightly increased order in the head-group region (C_2–C_5, Fig. 18b). At intermediate (12 Å<r<16 Å) and larger (22 Å<r<25 Å) distances, ordering in the tail group region of the 16:0 chain exceeds that of r>25 Å, i.e., the data lies above unity. For the 18:1c9 chain, disorder in the tail region is similarly closest to and most distant from the protein.

Therefore, in GlpF/POPC both 16:0 and 18:1c9 chains bend and/or tilt at the protein interface, in contrast to in GlpF/POPE where only the 18:1c9 chain bends and/or tilts near the protein, demonstrating that different structural responses are featured in the two bilayer types while satisfying hydrophobic matching.

6.5. Tilt order profiles

In order to examine the radially resolved lipid tilt order profiles for GlpF/POPE and GlpF/POPC, we diagonalized for each lipid molecule the radially resolved intertia tensor $\mathcal{I}(r)$

$$\langle \mathcal{I}'(r) \rangle = \langle \lambda^{-1} \mathcal{I}(r) \lambda \rangle_{N_i,t}. \tag{11}$$

Time and ensemble averages are indicated by $\langle \ldots \rangle_{t,Ni \in r}$ (omitted in the following) and λ is the diagonalizing matrix.

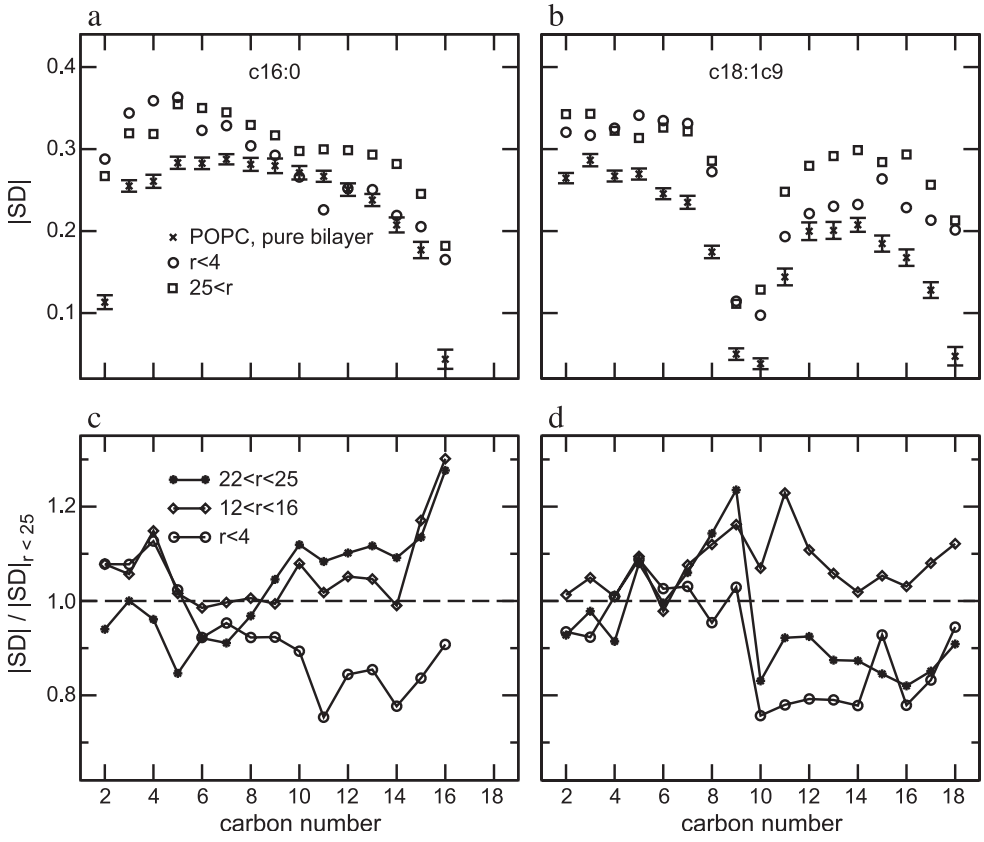

Fig. 18. (a, b) Radially resolved lipid order parameter profiles for GlpF/POPC for the 16:0 and 18:1c9 lipid acyl chains in selected (r<4 Å, r>25 Å) radial distances from the protein. (c, d) Selected (r<4 Å, 12 Å<r<16 Å, 22 Å<r<25 Å) GlpF/POPC order parameter profiles in (a, b) normalized by the appropriate r>25 Å data from (a, b).

All lipid atoms contributed while constructing the inertia tensor $\mathcal{I}_i(r)$ of the ith lipid molecule at distance r from the protein. Correspondingly,

$$\left(\langle\mathcal{I}'(r)\rangle-\langle E(r)\rangle\right)\langle\mathbf{I}(r)\rangle=0,\ \mathbf{I}(r)\equiv\left\{I_1(r),I_2(r),I_3(r)\right\} \tag{12}$$

yields time and ensemble averaged eigenvectors $\langle\mathbf{I}(r)\rangle$ (i.e., directors) and eigenvalues $\langle E(r)\rangle$ resolved radially from the protein. Within a rigid body approximation, we use these to determine the degree of tilt.

Results in terms of $\langle E(r)\rangle$ and $\langle\mathbf{I}(r)\rangle$ are shown in Fig. 19a and b, respectively, for GlpF/POPE and GlpF/POPC. Eigenvalues (Fig. 19a) for GlpF/POPC are larger than for GlpF/POPE regardless of moment of inertia due to the larger mass of the PC methyl groups relative to that of the PE groups. Eigenvalues are similar for I_1 and I_2 and larger than the eigenvalues for I_3. We identify the principal axis associated with the lowest moment of inertia I_3 as the long axis of the lipid molecule and therefore as the director of main interest. Next to the protein ($r\rightarrow 0$), the z-projection of the associated eigenvector in GlpF/POPE and GlpF/POPC (Fig. 19b) differs characteristically within a distance reaching about 6 Å. We conclude that some degree of lipid tilt is present in both systems within that distance and that more tilt is seen for GlpF/POPE (smaller z-projection of I_3). However, in the vicinity of the protein, a curling up of the lipid tail might also contribute to the hydrophobic matching mechanism. This effect will reduce static order near the protein (see Figs. 17 and 18) and increase the lowest moment of inertia, thus making I_3 approach the two larger moments of inertia (I_1, I_2). Near the protein we recall that static order is reduced for the 18:1c9 chain in GlpF/POPE and for both chains in GlpF/POPC. Therefore, both curling up of the acyl chains and tilt are determinants for the adjustment of the lipid molecules in the vicinity of the protein. Given the magnitude of the root-mean-square fluctuations in the eigenvectors in Fig. 19b, it cannot be settled, however, which one of the two structural responses is the major determinant for lipid adjustment at the protein interface.

6.6. Modulation of water transport by hydrophobic matching

In order to quantify concerted water diffusion occurring in single file through the water pores of GlpF (see Figs. 13 and 14), we have calculated, as a function of time and along

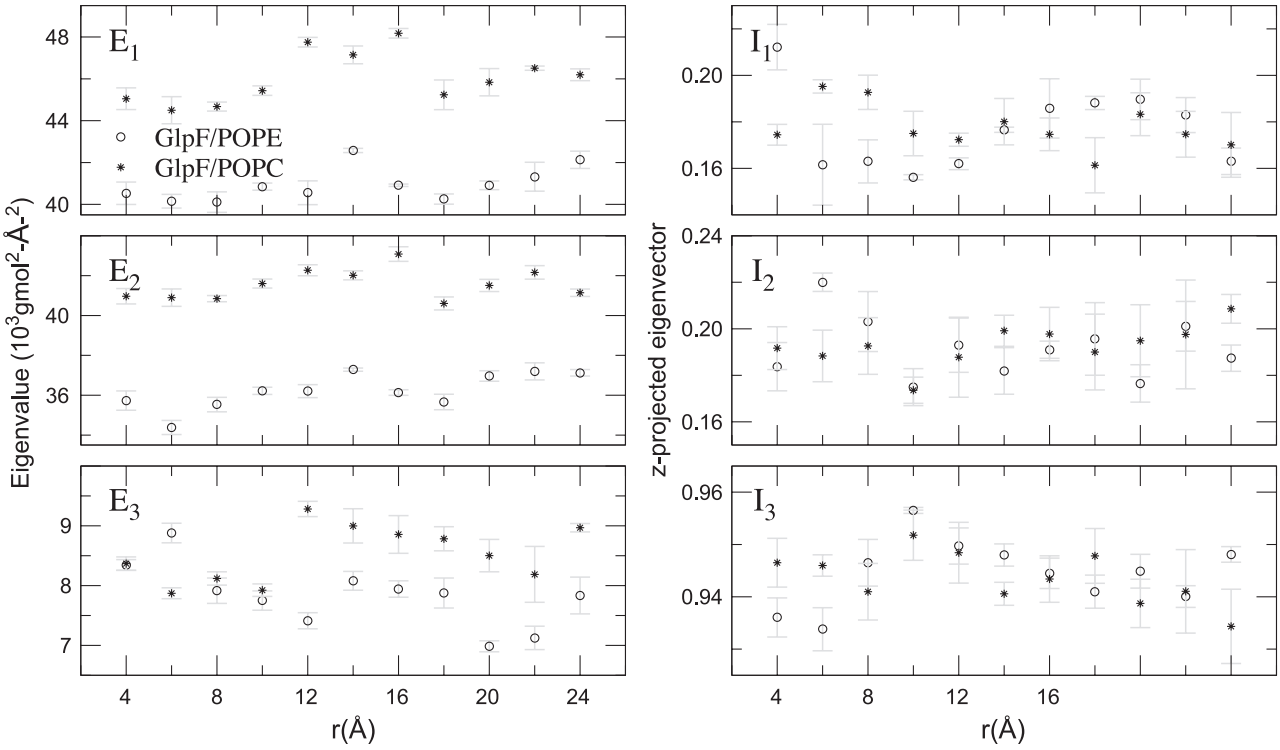

Fig. 19. Radially resolved lipid tilt for GlpF/POPE and GlpF/POPC. In calculating the tilt in a rigid body approximation, the average lipid director, resolved radially from the protein, was obtained by diagonalizing the inertia tensor, $\mathcal{I}_i(r)$, of the ith lipid molecule and subsequently averaging eigenvectors and eigenvalues over all lipid molecules $N_i \in r$ at time t and finally over time (last 2 ns of the simulations). Ensemble- and time-averaged eigenvectors and eigenvalues of the diagonalized intertia tensor $\mathcal{I}'(r)$ provide, respectively, an average magnitude of the three average lipid directors resolved radially from the protein; see Eqs. (11) and (12). We identify the principal axis associated with the lowest moment of inertia as the director of primarily interest. Variation of its projection onto the fixed surface normal (directed along z) along r is therefore our main indicator of tilt. We find that next to the protein ($r \to 0$), the z-projections of the associated eigenvector (I_3) in GlpF/POPE and GlpF/POPC differ characteristically, i.e., the lipid molecules tilt within a distance of about 6 Å.

the channel axis (z), the mean-square displacement (MSD) of the water molecules translocating concertedly in single file as

$$\mathrm{MSD}(t) = \frac{1}{N_{t'}} \sum_{t',i} \frac{1}{n_{\in \mathrm{CR}}(t',t)} [(z_i(t') - z_i(t'+t)]^2. \qquad (13)$$

$N_{t'}$ is here the number of gliding time origins and $n_{\in \mathrm{CR}}(t',t)$ is the number of water molecules within the constriction region (CR $\equiv -6$ Å $< z < 14$ Å; see Figs. 13 and 14) at time $t'+t$. Any water molecule diffusing outside the constriction region within a given time window initiated at t' is ignored in the remaining part of the calculation within that time window. The results are shown in Fig. 20.

As seen from Fig. 20, the MSD is approximately linear in time. The steepest slope occurs for GlpF/POPE. Using linear regression, we deduce the one-dimensional diffusion constants as $D = \Delta\mathrm{MSD}/2\Delta t$ yielding 0.42×10^{-5} cm^2/s (GlpF/POPE) and 0.33×10^{-5} cm^2/s (GlpF/POPC) with regression errors in D less than 10^{-7} cm^2/s. (Root-mean-square fluctuations in D among the individual monomers will be larger [70].) Since the simulations are equilibrium MD simulations carried out using periodic boundary conditions, the diffusion constants reflect thermally driven bidirectional water conduction [70], occurring faster in GlpF/POPE than in GlpF/POPC.

A continuous-time random-walk model developed for correlated water transport in carbon nanotubes [85,86] can be adopted to quantify single file water transport in aquaporins in full detail [70,87]. The key parameter in this model is the mean hopping time $\sigma = \bar{a}(2D)^{-1}$ for a concerted translocation (hop) of the water file by an amount equal to the average water–water separation- ($\bar{a}$) between the single-file water molecules. We find $\sigma = 114.4$ ps for (GlpF/POPE) and $\bar{\sigma} = 145.6$ ps (GlpF/POPC), using $\bar{a} = 3.1 \pm 0.2$ Å calculated from our simulations and the deduced values for D manifesting a faster water permeation in GlpF/POPE than in GlpF/POPC. Ultimately, this finding can be translated into the number of bidirectional permeation events per unit time (k) as given by [70,85,86] $k = [\bar{\sigma}(\bar{n}+1)]^{-1}$ with $\bar{n} = 7 \pm 1$ being the average occupancy of the constriction region. We find $k_{\mathrm{GlpF/POPE}}/k_{\mathrm{GlpF/POPC}} = 1.22$, i.e., more conduction events occur in GlpF/POPE. The absolute number of permeating water molecules $k_{\mathrm{GlpF/POPE}} = 1.1$/ns and $k_{\mathrm{GlpF/POPC}} = 0.9$/ns are, however, both within the accuracy of experimental data on permeation in aquaporins [88–90].

Our main point is that the conduction in GlpF/POPE is ~20% increased over that in GlpF/POPC. We can attribute this finding to a persistent increase of the channel radius in

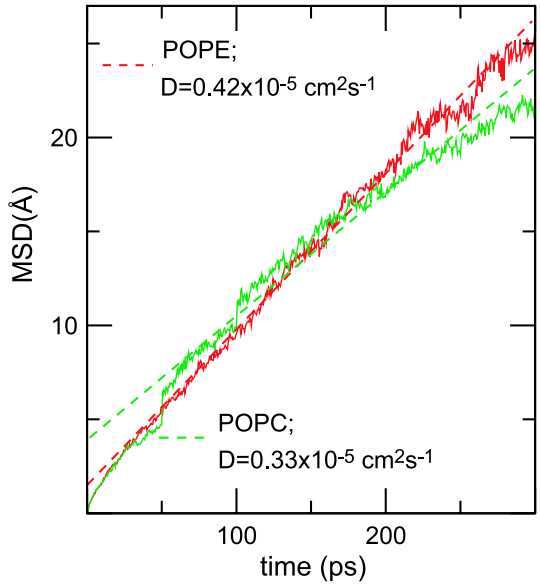

Fig. 20. Water permeation characteristics of the channel investigated by plotting the mean-square deviation (MSD), cf. Eq. (13), vs. time. Average one-dimensional diffusion constant (D) with a linear regression line providing one-dimensional diffusion constants through the constriction region (see Fig. 13) of 0.42×10^{-5} cm^2/s (GlpF/POPE) and 0.33×10^{-5} cm^2/s (GlpF/POPC) with regression errors in D less than 10^{-7} cm^2/s noting that root-mean-square fluctuations in D among the individual monomers will be larger [70]. A continuous-time random-walk model developed for correlated water transport in carbon nano-tubes [85,86] can be adopted to quantify single file-water transport in aquaporins in detail [70,87]. The key parameter in this model is the mean hopping time, $\bar{\sigma}=\bar{a}(2D)^{-1}$, for a concerted translocation (hop) of the water file by an amount equal to the average water–water separation ($\bar{a}$) between the single file water molecules. We find $\bar{\sigma}$ =114.4 ps for (GlpF/POPE) and $\bar{\sigma}$ =145.6 ps (GlpF/POPC), using $\bar{a}$=3.1±0.2 Å as calculated from our simulations and the appropriate values for D deduced from the linear regression. The corresponding number of water molecules passing the channel per unit time (k) is in turn given by [70,85] $k=[\bar{\sigma}(\bar{n}+1)]^{-1}$ with $\bar{n}$=7±1 being the average occupancy of the channel and equals 1.1/ns and 0.9/ns for GlpF/POPE and GlpF/POPC, respectively, which is within the accuracy of experimental data [88–90].

GlpF/POPC (about 10% through the entire channel, estimated using the program HOLE [91]; data not shown) caused by a change in lateral stress owing to the larger head group size of POPC relative to POPE as alluded in part in Section 4. The increased channel radius implies reduced water–water correlation (data not shown) which in turn lowers the probability for a concerted hopping event of the water wire, i.e., $\bar{\sigma}_{\mathrm{GlpF/POPC}} > \bar{\sigma}_{\mathrm{GlpF/POPE}}$. Despite GlpF being a remarkably stiff protein [65,70], we surprisingly find that the narrowest part of the channel denoted the selectivity filter region [67] (residues Trp48, Phe200, and Arg206), which also constitutes the main free energy barrier for water permeation [70], allows for reduced fluctuation in GlpF/POPC, and, consequently, also contributes to the lower permeation of water molecules per unit time in GlpF/POPC relative to GlpF/POPE. In closing, it should be noted that the results reported above for the conductance properties of GlpF are based on an analysis using a specific model, the CTRW model. Moreover, the number of permeation events obtained for GlpF/POPE and GlpF/POPC pertain to water-, protein-, and membrane-dynamics during a 5 ns time scale. In addition to the time-scale confinement and inherent assumptions of the CTRW model (e.g., fully correlated translocation of the single file), protein-lipid complexes might further exhibit sensitivity to, e.g., initial conditions and finite size of the systems. Therefore one cannot rule out that the respective permeation characteristics for GlpF embedded in the two membrane types might prove to be different at longer time scales or when not deduced from the CTRW model. This issue will be discussed further in Ref. [62].

7. Final words

It is expected that the quantitative study of lipid–protein interactions will be intensified in the near future as new nanoscopic experimental techniques get refined and as more realistic computer-simulation calculations become feasible. The growing number of resolved three-dimensional membrane protein structures [92] provides an improved basis for detailed and quantitative studies geared towards an understanding of the interplay between lipid-membrane structure and protein function. In addition, novel approaches may lead to new insight into the nature of the molecular structure and composition of the lipid–protein interface, e.g., by use of photochemical cross-linking principles [93]. By these techniques it will become possible to catch the lipids in the act, so to speak, and subsequently identify them by mass-spectroscopic techniques. Once the full details of lipid–protein interactions have been worked out, it will also become possible to assess the scientific basis for raft formation and raft function in biological membranes as well as to investigate the mechanisms of protein transport, protein translocation, and protein insertion into membranes.

Finally, it should be remarked that almost all studies of lipid–protein interactions reported refer to some kind of artificial equilibrium conditions to which thermodynamic principles can be applied. Obviously, a biologically functioning membrane system is not in thermodynamic equilibrium, but rather far from equilibrium or possible in a steady state controlled by fluxes of matter and energy. The consequences of lipid–protein interactions and the way they lead to organization of the membrane under these non-equilibrium conditions are so far only very little understood. However, it is clear that we are in for some surprises: the properties of the nonequilibrium driven or active membrane systems [94,95] may turn out to be very different from those characterizing equilibrium.

Acknowledgments

This work was supported by the Danish National Research Foundation via a grant to MEMPHYS-Center

for Biomembrane Physics. The simulations were in part carried out at the Danish Center for Scientific Computing (DCSC).

References

[1] E. Sackmann, Physical basis for trigger processes and membrane structures, in: D. Chapman (Ed.), Biological Membranes, vol. 5, Academic Press, London, 1984, pp. 105–143.
[2] S. Singer, G.L. Nicolson, The fluid mosaic model of cell membranes, Science 172 (1972) 720–730.
[3] J.N. Israelachvili, Refinements of the fluid-mosaic model of membrane structure, Biochim. Biophys. Acta 469 (1977) 221–225.
[4] D.W. Hilgeman, Getting ready for the decade of the lipids, Annu. Rev. Physiol. 65 (2003) 697–700.
[5] H.A. Rinia, B. de Kruijff, Imaging domains in model membranes with Atomic Force Microscopy, FEBS Lett. 504 (2001) 194–199.
[6] T. Kaasgaard, O.G. Mouritsen, K. Jørgensen, Lipid domain formation and ligand–receptor distribution in lipid bilayer membranes investigated by atomic force microscopy, FEBS Lett. 515 (2002) 29–34.
[7] L.A. Bagatolli, Direct observation of lipid domains in free standing bilayers: from simple to complex lipid mixtures, Chem. Phys. Lipids 122 (2003) 137–145.
[8] J. Bernardino de la Serna1, J. Perez-Gil, A.C. Simonsen, L.A. Bagatolli, Coexistence of fluid phases in native pulmonary surfactant membranes: cholesterol rules, J. Biol. Chem. (2004), in press.
[9] F. Oesterhelt, D. Oesterhelt, M. Pfeiffer, A. Engel, H.E. Gaub, D.J. Müller, Unfolding pathways of individual bacteriorhodopsins, Science 288 (2000) 143–146.
[10] S. Scheuring, D.J. Müller, H. Stahlberg, H.A. Engel, A. Engel, Sampling the conformational space of membrane protein surfaces with the AFM, Eur. Biophys. J. 31 (2002) 172–178.
[11] M. Edidin, The state of lipid rafts: from model membranes to cells, Annu. Rev. Biomol. Struct. 32 (2003) 257–283.
[12] R.G.W. Anderson, K. Jacobson, A role for lipid shells in targeting proteins to caveolae, rafts, and other lipid domains, Science 296 (2002) 1821–1825.
[13] O.G. Mouritsen, O.S. Andersen (Eds.), Search of a New Biomembrane Model, Biol. Skr. Dan. Vid. Selsk., vol. 49, 1998, pp. 1–214.
[14] O.G. Mouritsen, K. Jørgensen, Dynamical order and disorder in lipid bilayers, Chem. Phys. Lipids 73 (1994) 3–26.
[15] L.O. Bergelson, K. Gawrisch, J.A. Ferretti, F. Blumenthal (Eds.), Domain Organization in Biological Membranes. Mol. Membr. Biol. 12 (1995) 1–162.
[16] O.G. Mouritsen, Self-assembly and organization of lipid–protein membranes, Curr. Opin. Colloid Interface Sci. 3 (1998) 78–87.
[17] P.K.J. Kinnunen, On the principles of functional ordering in biological membranes, Chem. Phys. Lipids 57 (1991) 375–399.
[18] O.G. Mouritsen, M. Bloom, Mattress model of lipid–protein interactions in membranes, Biophys. J. 46 (1984) 141–153.
[19] T. Gil, J.H. Ipsen, O.G. Mouritsen, M.C. Sabra, M.M. Sperotto, M.J. Zuckermann, Theoretical analysis of protein organization in lipid membranes, Biochim. Biophys. Acta 1376 (1998) 245–266.
[20] F. Dumas, M.C. Lebrun, J.-F. Tocanne, Is the protein/lipid hydrophobic matching principle relevant to membrane organization and functions? FEBS Lett. 458 (1999) 271–277.
[21] A.N.J.A. Ridder, W. van de Hoef, J. Stam, A. Kuhn, B. de Kruijff, J.A. Killian, Importance of hydrophobic matching for spontaneous insertion of a single-spanning membrane protein, Biochemistry 41 (2002) 4946–4952.
[22] H. Hong, L.K. Tamm, Elastic coupling of integral membrane protein stability to lipid bilayer forces, Prof. Natl. Acad. Sci. U. S. A. 101 (2004) 4065–4070.
[23] O.G. Mouritsen, M.M. Sperotto, Thermodynamics of lipid–protein interactions in lipid membranes, in: M. Jackson (Ed.), Thermodynamics of Membrane Receptors and Channels, CRC Press, Boca Raton, FL, 1993, pp. 127–181.
[24] O.G. Mouritsen, M. Bloom, Models of lipid–protein interactions in membranes, Annu. Rev. Biophys. Biomol. Struct. 22 (1993) 145–171.
[25] F. Dumas, M.M. Sperotto, J.-F. Tocanne, O.G. Mouritsen, Molecular sorting of lipids by bacteriorhodopsin in DMPC–DSPC lipid bilayers, Biophys. J. 73 (1997) 1940–1953.
[26] A.G. Lee, Lipid–protein interactions in biological membranes: a structural perspective, Biochim. Biophys. Acta 1612 (2003) 1–40.
[27] R.S. Cantor, The influence of membrane lateral pressures on simple geometric models of protein conformational equilibria, Chem. Phys. Lipids 101 (1999) 45–56.
[28] O.G. Mouritsen, K. Jørgensen, A new look at lipid-membrane structure in relation to drug research, Pharm. Res. 15 (1998) 1507–1519.
[29] R.S. Cantor, The lateral pressure profile in membranes: a physical mechanism of general anesthesia, Biochemistry 36 (1997) 2339–2344.
[30] R.S. Cantor, Receptor desensitization by neurotransmitters in membranes: are neutransmitters the endogenous anesthetics? Biochemistry 42 (2003) 11891–11897.
[31] R.L. Goforth, A.K. Chi, D.V. Greathouse, L.L. Providence, R.E. Koeppe II, O.A. Andersen, Hydrophobic coupling of lipid bilayer energetics to channel function, J. Gen. Physiol. 121 (2003) 477–493.
[32] B. Martinac, O.P. Hamill, Gramicidin A channels switch between stretch activation and stretch inactivation depending on bilayer thickness, Proc. Natl. Acad. Sci. U. S. A. 99 (2003) 4308–4312.
[33] J.A. Killian, Synthetic peptides as models for intrinsic membrane proteins, FEBS Lett. 555 (2003) 134–138.
[34] T.M. Weiss, P.C.A. van der Wel, J.A. Killian, R.E. Koeppe II, H.W. Huang, Hydrophobic mismatch between helices and lipid bilayers, Biophys. J. 84 (2003) 379–385.
[35] M.M.R. de Planque, J.A. Killian, Protein–lipid interactions studied with designed transmembrane peptides: role of hydrophobic matching and interfacial anchoring, Mol. Membr. Biol. 20 (2003) 271–284.
[36] M.M.R. de Planque, B.B. Bonev, J.A.A. Demmers, D.V. Greathouse, R.E. Koeppe II, F. Separovic, A. Watts, J.A. Killian, Interfacial anchor properties of tryptophan residues in transmembrane peptides can dominate over hydrophobic matching effects in peptide–lipid interactions, Biochemistry 42 (2003) 5341–5348.
[37] H.I. Petrache, D.M. Zuckerman, J.N. Sachs, J.A. Killian, R.E. Koeppe II, T.B. Wollf, Hydrophobic matching mechanism investigated by molecular dynamics simulations, Langmuir 18 (2002) 1340–1351.
[38] T.A. Harroun, W.T. Heller, T.M. Weiss, L. Yang, H.W. Huang, Experimental evidence for hydrophobic matching and membrane-mediated interactions in lipid bilayers containing gramicidin, Biophys. J. 76 (1999) 937–945.
[39] J.A. Lundbæk, O.S. Andersen, Lysophospholipids modulate challel function by altering the mechanical properties of lipid bilayers, J. Gen. Physiol. 104 (1994) 645–673.
[40] T.-C. Hwang, R.E. Koeppe II, O.S. Andersen, Genistein can modulate channel function by a phosphorylation-independent mechanism: importance of hydrophobic mismatch and bilayer mechanics, Biochemistry 42 (2003) 13646–13658.
[41] O.S. Andersen, C. Nielsen, A.M. Maer, J.A. Lundbæk, M. Goulian, R.E. Koeppe II, Ion channels as tools to monitor lipid bilayer–membrane protein interactions: gramicidin channels as molecular force transducers, Methods Enzymol. 294 (1998) 208–224.
[42] F. Dumas, J.F. Tocanne, G. Leblanc, M.C. Lebrun, Consequences of hydrophobic mismatch between lipids and melibiose permease on melibiose transport, Biochemistry 39 (2000) 4846–4854.
[43] F. Cornelius, Modulation of Na,K-ATPase and Na-ATPase activity by phospholipids and cholesterol: I. Steady-state kinetics, Biochemistry 40 (2001) 8842–8851;
F. Cornelius, N. Turner, H.R.Z. Christensen, Modulation of Na,K-ATPase by phospholipids and cholesterol: II. Steady-state and pre-steady-state kinetics, Biochemistry 42 (2003) 8541–8549.
[44] S. Munro, Localization of proteins to the Golgi apparatus, Trends Cell Biol. 8 (1998) 11–15.

[45] R.S. Cantor, Lateral pressures in cell membranes: a mechanism for modulation of protein function, J. Phys. Chem. 101 (1997) 1723–1725.
[46] S. Gruner, Lipid membrane curvature elasticity and protein function, in: L. Peliti (Ed.), Biologically Inspired Physics, Plenum, New York, 1991, pp. 127–135.
[47] P.K.J. Kinnunen, On the mechanisms of the lamellar→hexagonal H_{II} phase transition and the biological significance of H_{II} propensity, in: D. Lasic, Y. Barenholz (Eds.), Nonmedical Applications of Liposomes, CRC Press, Boca Raton, FL, 1995, pp. 153–171.
[48] R. Epand, Lipid polymorphism and protein–lipid interactions, Biochim. Biophys. Acta 1376 (1998) 353–368.
[49] P.K.J. Kinnunen (Ed.), Peripheral Interactions on Lipid Surfaces: Towards a New Biomembrane Model. Chem. Phys. Lipids 101 (1999) 1–137.
[50] A. Hinderliter, A.R.G. Dibble, R.L. Biltonen, J.J. Sando, Activation of protein kinase C by coexisting diacylglycerol-enriched and diacylglycerol-poor lipid domains, Biochemistry 36 (1996) 6141–6148.
[51] E.K.J. Tuominen, C.J.A. Wallace, P.K.J. Kinnunen, Phospholipid–cytochrome *c* interaction. Evidence for the extended lipid anchorage, J. Biol. Chem. 277 (2002) 8822–8826.
[52] M.F. Brown, Influence of non-lamellar-forming lipids on rhodopsin, Curr. Top. Membr. 44 (1997) 285–356.
[53] D.C. Mitchell, J.T.R. Lawrence, B.J. Litman, Primary alcohols modulate the activation of the G protein-coupled receptor rhodopsin by a lipid-mediated mechanism, J. Biol. Chem. 271 (1996) 19033–19036.
[54] S.I. Sukharev, P. Blount, B. Martinac, C. Kung, Mechanosensitive channels of *Escherichia coli*: the MscL gene, protein, and activities, Annu. Rev. Physiol. 59 (1997) 633–657.
[55] E. Perozo, A. Kloda, D.M. Cortes, B. Martinac, Physical principles underlying the transduction of bilayer deformation forces during mechanosensitive channel gating, Nat. Struct. Biol. 9 (2002) 696–703.
[56] J. Gullingsrud, D. Kosztin, K. Schulten, Structural determinants of Mscl gating studied by molecular dynamics simulations, Biophys. J. 80 (2001) 2074–2081.
[57] J. Gullingsrud, K. Schulten, Lipid bilayer pressure profiles and mechanosensitive channel gating, Biophys. J. 86 (2004) 2883–2895.
[58] J.A. Killian, G. von Heijne, How proteins adapt to a membrane–water interface, Trends Biochem. Sci. 25 (2000) 429–434.
[59] C. Nielsen, O.S. Andersen, Energetics of inclusion-induced bilayer deformatiosn, Biophys. J. 74 (1998) 1966–1983.
[60] T.A. Harroun, W.T. Heller, T.M. Weiss, L. Yang, H.W. Huang, Theoretical analysis of hydrophobic matching and membrane-mediated interactions in lipid bilayers containing gramicidin, Biophys. J. 76 (1999) 3176–3185.
[61] C. Nielsen, O.S. Andersen, Inclusion-induced bilayer deformations: effects of monolayer equilibrium curvature, Biophys. J. 79 (2000) 2583–2604.
[62] M.Ø. Jensen, O.G. Mouritsen. Direct observation of hydrophobic matching between lipids and proteins in membranes (preprint, 2004).
[63] P. Agre, The aquaporins, blueprints for cellular plumbing systems, J. Biol. Chem. 273 (1998) 14659–14662.
[64] K.B. Heller, E.C. Lin, T.H. Wilson, Substrate specificity and transport properties of the glycerol facilitator of *Escherichia coli*, J. Bacteriol. 144 (1980) 274–278.
[65] M.Ø. Jensen, E. Tajkhorshid, K. Schulten, The mechanism of glycerol conduction in aquaglyceroporins, Structure 9 (2001) 1083–1093.
[66] M.Ø. Jensen, S. Park, E. Tajkhorshid, K. Schulten, Energetics of glycerol conduction through aquaglyceroporin GlpF, Proc. Natl. Acad. Sci. U. S. A. 99 (2002) 6731–6736.
[67] D. Fu, A. Libson, L.J.W. Miercke, C. Weitzman, P. Nollert, J. Krucinski, R.M. Stroud, Structure of a glycerol conducting channel and the basis for its selectivity, Science 290 (2000) 481–486.
[68] P. Grayson, E. Tajkhorshid, K. Schulten, Mechanisms of selectivity in channels and enzymes studied with interactive molecular dynamics, Biophys. J. 85 (2003) 36–48.
[69] D. Lu, P. Grayson, K. Schulten, Glycerol conductance and physical asymmetry of the *Escherichia coli* glycerol facilitator GlpF, Biophys. J. 85 (2003) 2977–2987.
[70] M.Ø. Jensen, E. Tajkhorshid, K. Schulten, Electrostatic control of permeation and selectivity in aquaporins, Biophys. J. 85 (2003) 2884–2899.
[71] E. Tajkhorshid, P. Nollert, M.Ø. Jensen, L.J.W. Miercke, J. O'Connell, R.M. Stroud, K. Schulten, Control of the selectivity of the aquaporin water channel family by global orientational tuning, Science 296 (2002) 525–530.
[72] N. Chakrabarti, E. Tajkhorshid, B. Roux, R. Poms, Molecular basis of proton blockage in aquaporins, Structure 12 (2004) 65–74.
[73] B.L. de Groot, H. Grubmüller, Water permeation through biological membranes: mechanism and dynamics of Aquaporin-1 and GlpF, Science 294 (2001) 2353–2357.
[74] H. Grubmüller, Solvate 1.0, 1996, http://www.mpibpc.gwdg.de/abteilungen/071/solvate/docu.html.
[75] L. Kalé, R. Skeel, M. Bhandarkar, R. Brunner, A. Gursoy, N. Krawetz, J. Phillips, A. Shinozaki, K. Varadarajan, K. Schulten, NAMD2: greater scalability for parallel molecular dynamics, J. Comp. Physiol. 151 (1999) 283–312.
[76] M. Schlenkrich, J. Brickmann, A. MacKerell Jr., M. Karplus, Empirical potential energy function for phospholipids: criteria for parameter optimization and applications, in: K.M. Merz, B. Roux (Eds.), Biological Membranes: A Molecular Perspective from Computation and Experiment, Birkhauser, Boston, 1996, pp. 31–81.
[77] S.E. Feller, A. MacKerell, An improved empirical potential energy function for molecular simulations of phospholipids, J. Phys. Chem. 104 (2000) 7510–7515.
[78] T. Darden, D. York, L. Pedersen, Particle Mesh Ewald: An *N*log(*N*) method for Ewald sums in large systems, J. Chem. Phys. 98 (1993) 10089–10092.
[79] W. Humphrey, A. Dalke, K. Schulten, VMD—visual molecular dynamics, J. Mol. Graph. 14 (1996) 33–38.
[80] P. Høyrup, T.H. Callisen, M.Ø. Jensen, A. Halperin, O.G. Mouritsen, Lipid protrusions, membrane softness, and enzymatic activity, Chem. Phys. Phys. Chem. 6 (2004) 3556–3575.
[81] J. Cohen, K. Schulten, Mechanism of anionic conduction across ClC, Biophys. J. 86 (2004) 836–845.
[82] D.P. Tieleman, L.R. Forrest, M.S.P. Sansom, H.J.C. Berendsen, Lipid properties and the orientation of aromatic residues in OmpF, influenza and alamethicin systems: molecular dynamics simulations, Biochemistry 37 (1999) 17554–17561.
[83] A.M. Maer, L.L. Providence, C. Nielsen, O.S. Andersen, Gramicidin A channel's behavior in bilayers made of lipid mixtures, Biophys. J. 74 (1998) A203.
[84] M. Bloom, E. Evans, O.G. Mouritsen, Physical properties of the fluid-bilayer component of cell membranes: a perspective, Q. Rev. Biophys. 24 (1991) 293–397.
[85] A. Berezhkovskii, G. Hummer, Single-file transport of water molecules through a carbon nanotube, Phys. Rev. Lett. 89 (2002) 064503-1–064503-4.
[86] F. Zhu, K. Schulten, Water and proton conduction through carbon nanotubes as models for biological channels, Biophys. J. 85 (2003) 236–244.
[87] F. Zhu, E. Tajkhorshid, K. Schulten, Theory and simulation of water permeation in aquaporin-1, Biophys. J. 86 (2004) 50–57.
[88] J.B. Haymann, A. Engel, Aquaporins: phylogeny, structure and physiology of water channels, News Physiol. Sci. 14 (1999) 187–194.
[89] M. Borgnia, S. Nielsen, A. Engel, P. Agre, Cellular and molecular biology of the aquaporin water channels, Annu. Rev. Biochem. 68 (1999) 425–458.
[90] M.J. Borgnia, P. Agre, Reconstitution and functional comparison of purified GlpF and AqpZ, the glycerol and water channels from *Escherichia coli*, Proc. Natl. Acad. Sci. U. S. A. 98 (2001) 2888–2893.

[91] O.S. Smart, J.G. Neduvelil, X. Wang, B.A. Wallace, M.S.P. Sansom, HOLE: a program for the analysis of the pore dimensions of ion channel structural models, J. Mol. Graph. 14 (1996) 354–360.
[92] See http://www.mpibp-frankfurt.mpg.de/michel/public/memprotstruct.html for a list of known membrane protein structures.
[93] A. Ridder, et al., Photo-crosslinking analysis of preferential interactions between a transmembrane peptide and matching lipids, Biochemistry 43 (2004) 4482–4489.
[94] M.C. Sabra, O.G. Mouritsen, Steady-state compartmentalization of lipid membranes by active proteins, Biophys. J. 74 (1998) 745–752.
[95] J.-B. Manneville, P. Bassereau, S. Ramaswamy, J. Prost, Active membrane fluctuations studied by micropipet aspiration, Phys. Rev., E 64 (2001) 021908–021910.
[96] O.G. Mouritsen, Life as a Matter of Fat. The Emerging Science of Lipidomics, SpringerVerlag, Heidelberg, 2005.